Journal of Organometallic Chemistry 854 (2018) 49–63

Contents lists available at ScienceDirect

Journal of Organometallic Chemistry

journal homepage: www.elsevier.com/locate/jorganchem

Synthesis, characterization and biological applications of substituted pyrazolone core based platinum(II) organometallic compounds

Miral V. Lunagariya, Khyati P. Thakor, Darshana N. Kanthecha, Mohan N. Patel*

Department of Chemistry, Sardar Patel University, Vallabh Vidyanagar, 388 120, Gujarat, India

ARTICLE INFO

Article history:
Received 22 June 2017
Received in revised form
8 November 2017
Accepted 11 November 2017
Available online 15 November 2017

Keywords:
Organometallic platinum(II) compounds
2-Phenyl-5-methyl pyrazolone based ligands
In vitro cytotoxicity
DNA interaction study
DNA cleavage assay

ABSTRACT

New series of organometallic platinum(II) compounds **(I-VI)** containing the 2-phenyl-5-methyl pyrazole-3-one derivatives ligands (L^1-L^6) were synthesized and characterized by spectroscopic and physico-chemical techniques. The synthesized compounds were screen for their *in vitro* antibacterial activity against two Gram$^{(+ve)}$ and three Gram$^{(-ve)}$ bacterial species. *In vitro* cytotoxicity against brine shrimp lethality bioassay and *in vitro* cellular level cytotoxicity against *S. pombe* cells were carried out for the synthesized compounds. Complexes (I-VI) exhibit excellent cytotoxicity as compared to ligands (L^1-L^6). DNA interaction and DNA cleavage study of the synthesized ligands and complexes were carried out using absorption titration spectroscopy, fluorescence quenching analysis, viscosity measurements, molecular docking study and agarose gel electrophoresis. The interactions of compounds towards herring sperm DNA (HS-DNA) was examined. The binding constant (K_b), Stern-Volmer quenching constant (K_{sv}) and associative binding constant (K_a) of the synthesized ligands and complexes were observed in the range of 0.138–5.580 × 10^5 M^{-1}, 1.1 × 10^2 to 7.0 × 10^3 M^{-1} and 1.871 × 10^3 to 1.711 × 10^5 M^{-1}, respectively. In molecular docking study, binding energy of compounds were observed in the range of −240.74 to −325.79 $kJmol^{-1}$. The results propose that all the compounds could interact with HS-DNA via the partial intercalative mode of binding.

1. Introduction

Since the discovery by Rosenberg, cisplatin (*cis*-diamminedichloroplatinum(II)) is one of the most general anticancer drugs encouraged the search for novel metal-based therapeutic agents in cancer [1,2]. There is still scope for the elimination of side effects (e.g. nausea, hearing loss, vomiting, etc.), higher solubility and the ability to use it in combination with other drugs [3]. Coordination compounds of transition metals describe a great history of their usefulness in the cure of various diseases [4–6]. The major application of these compounds finds use in the field of discovery of new anticancer agent. Various oxidation states exhibited by transition metals, find use as compounds interacting with a number of negatively charged molecules and thus leads to the development of metal-based drugs with surprising pharmacological purpose and may present exceptional curative opportunities. Metals can play an important role in modifying the pharmacological properties of ligands after its coordination to a ligand [7]. Chelation causes drastic change in biological properties of ligands as well as metal moiety and in many cases it causes synergistic effect of metal ion and ligand both. Organometallic platinum(II) complexes have been reported as anti-diabetic, anti-inflammatory, antimanic, antimicrobial, antiparasitic, antiulcer, antihypertensive agents [8].

Many pyrazole derivatives are well approved to possess a wide range of medicinally and biologically activities [9]. The heterocyclic molecules, which are present in many important drugs and agrochemical such as Celecoxib (antiarthritic), Mavacoxib (antiarthritic), Razaxaban (anticoagulant), Fluazolate (herbicide) and Penthiopyrad (fungicide) [10,11]. Despite of an extensive amount of literature on metal complex–DNA interaction, the information regarding the nature of binding of these complexes to DNA has remained a subject of extreme debate. The structure, size and relative nature of the ligands in the coordination complex has a direct influence on DNA binding [12].

Considering these aspects in mind, in present work, the synthesis of pyrazole derivatives ligands were carried out by conventional methods. And also synthesized organometallic platinum(II) complexes (I-VI) via dichloro bridge dimer as an intermediate. Biological activity of the synthesized ligands and complexes were

* Corresponding author.
E-mail address: jeenen@gmail.com (M.N. Patel).

https://doi.org/10.1016/j.jorganchem.2017.11.012
0022-328X/

carried out by performing *in vitro* cytotoxicity against brine shrimp lethality bioassay, *in vitro* cellular cytotoxicity against *S. pombe* cells, *in vitro* antibacterial activity against five different pathogen, electronic absorption titration spectroscopy, viscosity measurements, fluorescence quenching analysis, molecular docking and DNA nuclease activity.

2. Experimental section

2.1. Chemicals and reagents

Solvents were dried and distilled previous to their use following standard process [13]. All the chemicals were using of analytical grade. Ethidium bromide (EB), bromophenol blue, agarose and Luria Broth (LB) were purchased from Hi-media Laboratories Pvt. Ltd., India. Potassium tetrachloro platinate(II) salt, 4-tolualdehyde, 4-methoxy benzaldehyde, 4-hydroxy benzaldehyde, 4-chloro benzaldehyde, 4-bromo benzaldehyde, 4-nitro benzaldehyde and 2-phenyl-5-methyl-pyrazole-3-one were purchased from Sigma Chemical Co. (India) and were used as received without further purification. Culture of pUC19 bacteria (MTCC 47), two Gram$^{(+ve)}$, i.e. *Staphylococcus aureus* (*S. aureus*) (MTCC-3160) and *Bacillus subtilis* (*B. subtilis*) (MTCC-7193), and three Gram$^{(-ve)}$, i.e. *Serratia marcescens* (*S. marcescens*) (MTCC-7103), *Pseudomonas aeruginosa* (*P. aeruginosa*) (MTCC-1688) and *Escherichia coli* (*E. coli*) (MTCC-433), were purchased from Institute of Microbial Technology (Chandigarh, India). *S. pombe* Var. Paul Linder 3360 was obtained from IMTECH, Chandigarh. Ethidium bromide (EB) and pUC19 bacteria (MTCC 47) were used for all DNA binding and cleavage studies.

2.2. Physical measurements

Thermogravimetric analysis (TGA) was performed with a model SDT Q600 V20.9 Build 20, TA instrument (USA), to record curves under a nitrogen (N_2) atmosphere with a heating rate of 20 °C min^{-1} in the temperature range from 25 °C to 800 °C. The micro-elemental analysis (C, H, N and S) content of the compounds was carried out with a Euro Vector EA3000 elemental analyser (240). The magnetic moments were measured by Gouys method using mercury tetrathiocyanatocobaltate(II) as the calibrate ($\chi_g = 16.44 \times 10^{-6}$ cgs units at 20 °C). Melting points were determined on Buchi 540 melting point apparatus. Infrared spectra were recorded on a Perkin-Elmer FT IR Shimadzu model spectrophotometer using the KBr disc technique in the range of 4000–400 cm^{-1}. In the range of 200–800 nm, electronic absorption spectra were recorded using a UV-160A UV–Vis spectrophotometer Shimadzu, Kyoto (Japan), with a 10 mm path length quartz cell. Fluorescence spectra were recorded on a FluoroMax-4, spectrofluorometer, HORIBA (Scientific). The LC–MS spectra were recorded by thermo mass spectrophotometer (USA). Minimum concentration inhibitory study was carried out using laminar air flow cabinet, Toshiba, Delhi, (India). The ^{1}H NMR and ^{13}C NMR spectra were recorded on a Bruker Avance (400 MHz) and (100 MHz), respectively either in DMSO-d_6 (35 °C), referenced internally to the solvent. Photo quantization of the gel after electrophoresis was prepared by AlphaDigiDocTM RT. Version V.4.0.0 PC–Image software, CA (USA). Hydrodynamic chain length study was carried out by viscometric measurement bath.

2.3. General synthesis of the substituted 2-phenyl-5-methyl pyrazole-3-one based ligands (L^1–L^6)

To the solution of 5-methyl-2-phenyl-2,4-dihydro-3H-pyrazol-3-one (1 mmol) and different substituted benzaldehyde (1 mmol) with catalytic amount acetic acid (5 mL) was added in round bottom flask using ethanol solvent. The mixture was refluxed under stirring for 3 h. After completion of the reaction, the reaction mass was cooled, and then evaporated to dryness in vacuum. The reaction mixture extracted with ethyl acetate (3 × 5 mL). The combined ethyl acetate layers were back-extracted with saturated sodium bicarbonate (3 × 5 mL) and brine (3 × 5 mL), dried over $MgSO_4$, filtered, and evaporated in vacuum. The residue was crystallized from ethanol to obtain the target compounds. The proposed reaction scheme for the synthesized uninegative bidentate ligands (L^1-L^6) are represented in Scheme 1.

2.3.1. Structural characterization of (E)-5-methyl-4-(4-methylbenzylidene)-2-phenyl-2,4-dihydro-3H-pyrazol-3-one (L^1)

This ligand (L^1) was prepared through the addition of 2-phenyl-5-methyl pyrazole-3-one (1a) (522 mg, 3 mmol) and p-methyl benzaldehyde (2a) (360 mg, 3 mmol) and reflux for 5–6 h in presences of catalytic amount AcOH and EtOH solution as described in general process. **Colour:** yellowish powder, Yield: 85%, **mol. wt.:** 276.34 g/mol, **m.p.:** 125 °C; **Anal. Calc. (%) For $C_{18}H_{16}N_2O$:** C, 78.24; H, 5.84; N, 10.14. **Found (%):** C, 78.06; H, 5.65; N, 10.10. **UV-vis: λ(nm) (ε, M^{-1} cm^{-1}):** 256 (34,070), 288 (7160). **MS m/z (%):** 276.70 [M]. **^{1}H NMR (400 MHz, DMSO-d_6) δ/ppm:** 8.71 (2H, d, J = 8.8 Hz, $H_{2'',6''}$), 7.92 (2H, d, J = 8.0 Hz, $H_{2',6'}$), 7.76 (1H, s, H_6), 7.43 (3H, t, $^3J_1$ = 7.6 Hz, $^3J_2$ = 7.6 Hz, $H_{3'',4'',5''}$), 7.12–7.10 (2H, m, $H_{3',5'}$), 3.89 (3H, s, pyrazole-CH_3), 2.33 (3H, s, toluene ring-CH_3). **^{13}C NMR (100 MHz, DMSO-d_6) δ/ppm:** 165.52 (C=O, $C_{quat.}$), 147.58 (C_3, $C_{quat.}$), 143.45 (C_6,-CH), 140.34 ($C_{1''}$, $C_{quat.}$), 137.64 ($C_{4'}$, $C_{quat.}$), 134.43 ($C_{2',6'}$, -CH), 129.93 ($C_{1'}$,$C_{quat.}$), 128.99 ($C_{3',5'}$, -CH), 127.69 ($C_{3'',5''}$, -CH), 127.00 ($C_{4''}$, -CH), 126.27 (C_4, -$C_{quat.}$), 118.50 ($C_{2'',6''}$ -CH), 21.34 (-CH_3, phenyl ring), 15.05 (-CH_3, pyrazole). [**Total signal observed = 14:** signal of C = 6 (pyrazole-C = 3, phenyl ring-C = 3), signal of CH and CH_3 = 8 (substituted pyarazole-CH = 1, phenyl ring-CH = 5, pyrazole-CH_3 = 1, phenyl ring-CH_3 = 1]. **FT-IR (KBr): (cm^{-1}):** 3078 $\nu_{(=C-H)ar}$ (w), 1689 $\nu_{(-N-C=O)}$, 1514–1604 $\nu_{(C=N)}$ (s), 1426 $\nu_{(C=C)conjugated\ alkenes}$ (m), 1373 $\nu_{(C-H)banding}$ (m), 1319 $\nu_{(C-N)}$, 1195 $\nu_{(C-C)alkanes}$ (s), 763 $\nu_{(Ar-H)}$ 2 adjacent hydrogen (s).

2.3.2. Structural characterization of (E)-4-(4-methoxybenzylidene)-5-methyl-2-phenyl-2,4-dihydro-3H-pyrazol-3-one (L^2)

This ligand (L^2) was prepared through the addition of 2-phenyl-5-methyl pyrazole-3-one (1a) (522 mg, 3 mmol) and *p*-methoxy benzaldehyde (2b) (408 mg, 3 mmol) and reflux for 5–6 h in presences of catalytic amount AcOH and EtOH solution as described in general process. **Colour:** pale yellowish powder, **Yield:** 92%, **mol. wt.:** 292.34 g/mol, **m.p.:** 130 °C; **Anal. Calc. (%) For $C_{18}H_{16}N_2O_2$**: C, 73.95; H, 5.52; N, 9.58. **Found (%):** C, 73.10; H, 5.45; N, 9.30. **UV-vis: λ(nm) (ε, M^{-1} cm^{-1}):** 257 (37,260), 330 (17,690). **MS m/z (%):** 292.37 [M]. **^{1}H NMR (400 MHz, DMSO-d_6) δ/ppm:** 8.73 (2H, d, J = 8.0 Hz, $H_{2'',6''}$), 7.93 (2H, d, J = 7.6 Hz, $H_{2',6'}$), 7.92 (1H, s, H_6), 7.43 (3H, t, $^3J_1$ = 7.2 Hz, $^3J_2$ = 5.6 Hz, $H_{3'',4'',5''}$), 7.21–7.11 (2H, m, $H_{3',5'}$), 4.41 (3H, phenyl ring-CH_3), 2.34 (3H, pyrazole-CH_3). **^{13}C NMR (100 MHz, DMSO-d_6) δ/ppm:** 165.52 (C=O, $C_{quat.}$), 147.58 (C_3, $C_{quat.}$), 159.84 ($C_{4'}$,$C_{quat.}$), 143.45 (C_6,-CH.), 140.34 ($C_{1''}$, $C_{quat.}$), 130.23 ($C_{2',6'}$, -CH), 126.20 (C_4,$C_{quat.}$), 125.24 ($C_{1'}$, -CH), 128.99 ($C_{3'',5''}$, -CH), 128.00 ($C_{4''}$, -CH), 118.50 ($C_{2'',6''}$, -CH), 114.22 ($C_{3',5'}$ -CH), 55.81 (-OCH_3, phenyl ring), 15.05 (-CH_3, pyrazole). [**Total signal observed = 14:** signal of C = 6 (pyrazole-C = 3, phenyl ring-C = 3), signal of CH and CH_3 = 8 (substituted pyarazole-CH = 1, phenyl ring-CH = 5, pyrazole-CH_3 = 1, phenyl ring-OCH_3 = 1]. **FT-IR (KBr): (cm^{-1}):** 3078 $\nu_{(=C-H)ar}$ (w), 1674 $\nu_{(-N-C=O)}$, 1550–1589 $\nu_{(C=N)}$ (s), 1488 $\nu_{(C=C)conjugated\ alkenes}$ (m), 1365 $\nu_{(C-H)banding}$ (m), 1311 $\nu_{(C-N)}$, 1265 $\nu_{(C-C)alkanes}$ (s), 756 $\nu_{(Ar-H)2\ adjacent\ hydrogen}$ (s).

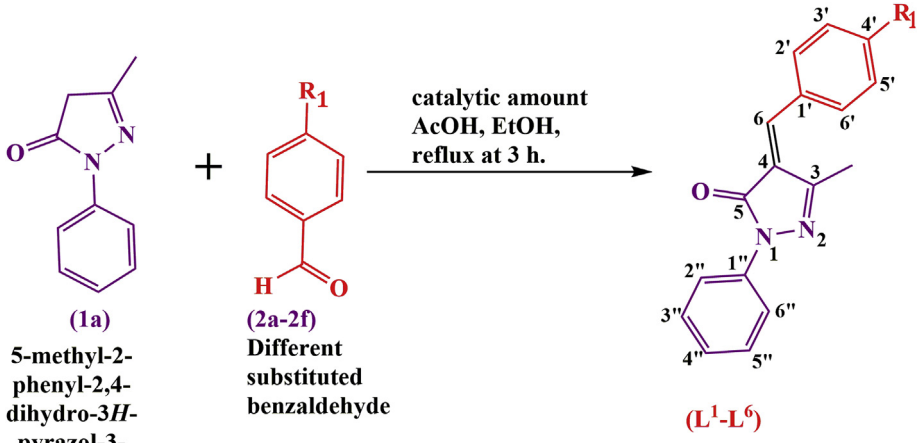

Ligands	R_1
L^1	$-CH_3$
L^2	$-OCH_3$
L^3	-OH
L^4	-Cl
L^5	-Br
L^6	$-NO_2$

Scheme 1. Synthesis of the different substituted 2-phenyl-5-methyl-pyrazol-3-one derivatives ligands ($L^1 - L^6$).

2.3.3. Structural characterization of (E)-4-(4-hydroxybenzylidene)-5-methyl-2-phenyl-2,4-dihydro-3H-pyrazol-3-one (L^3)

This ligand (L^3) was prepared through the addition of 2-phenyl-5-methyl pyrazole-3-one (1a) (522 mg, 3 mmol) and p-hydroxy benzaldehyde (2c) (366 mg, 3 mmol) and reflux for 5–6 h in presences of catalytic amount AcOH and EtOH solution as described in general process. **Colour:** orange powder, **Yield:** 88%, **mol. wt.:** 278.31 g/mol, **m.p.:** 135 °C; **Anal. Calc. (%) For $C_{17}H_{14}N_2O_2$:** C, 73.37; H, 5.07; N, 10.07. **Found (%):** C, 73.31; H, 5.05; N, 10.30. **UV-vis: λ(nm) (ε, M^{-1} cm^{-1}):** 254 (36,470), 288 (6390). **MS m/z (%):** 278.57 [M]. **^{1}H NMR (400 MHz, DMSO-d_6) δ/ppm:** 9.95 (1H, s, -OH), 8.74 (2H, d, $J = 8.0$ Hz, $H_{2'',6''}$), 7.93 (2H, d, $J = 8.0$ Hz, $H_{3',5'}$), 7.77 (1H, s, H_6), 7.43 (3H, t, $^3J_1 = 8.4$ Hz, $^3J_2 = 7.6$ Hz, $H_{3'',4'',5''}$), 7.21–7.11 (2H, m, $H_{2',6'}$), 2.34 (3H, pyrazole-CH_3). **^{13}C NMR (100 MHz, DMSO-d_6) δ/ppm:** 165.54 (C=O, $C_{quat.}$), 157.71 ($C_{4'}$, $C_{quat.}$), 147.53 (C_3,$C_{quat.}$), 143.40 (C_6,-CH.), 140.32 ($C_{1''}$, $C_{quat.}$), 130.68 ($C_{2',6'}$, -CH), 128.96 ($C_{3'',5''}$,-CH), 128.00 ($C_{4''}$, -CH), 126.25 (C_4, -CH), 125.55 ($C_{1'}$, -CH), 118.51 ($C_{2'',6''}$, -CH), 115.86 ($C_{3',5'}$ -CH), 15.22 (-CH_3, pyrazole). [**Total signal observed = 13:** signal of C = 6 (pyrazole-C = 3, phenyl ring-C = 3), signal of CH and CH_3 = 7 (substituted pyarazole-CH = 1, phenyl ring-CH = 5, pyrazole-CH_3 = 1]. **FT-IR (KBr): (cm^{-1}):** 3209 $\nu_{(\text{-O-H})}$, 3055 $\nu_{(\text{=C-H})\text{ar}}$ (w), 1658 $\nu_{(\text{-N-C=O})}$, 1550–1596 $\nu_{(\text{C=N})}$ (s), 1504 $\nu_{(\text{C=C})\text{conjugated alkenes}}$ (m), 1380 $\nu_{(\text{C-H})\text{banding}}$ (m), 1334 $\nu_{(\text{C-N})}$, 1296 $\nu_{(\text{C-C})\text{alkanes}}$ (s), 748 $\nu_{(\text{Ar-H})2\text{ adjacent hydrogen}}$ (s).

2.3.4. Structural characterization of (E)-4-(4-chlorobenzylidene)-5-methyl-2-phenyl-2,4-dihydro-3H-pyrazol-3-one (L^4)

This ligand (L^4) was prepared through the addition of 2-phenyl-5-methyl pyrazole-3-one (1a) (522 mg, 3 mmol) and *p*-chloro benzaldehyde (2d) (421 mg, 3 mmol) and reflux for 5–6 h in presences of catalytic amount AcOH and EtOH solution as described in general process. **Colour:** orange powder, **Yield:** 85%, **mol. wt.:** 296.75 g/mol, **m.p.:** 132 °C; **Anal. Calc. (%) For $C_{17}H_{13}ClN_2O$:** C, 68.81; H, 4.42; N, 9.44. **Found (%):** C, 68.31; H, 4.05; N, 9.30. **UV-vis: λ(nm) (ε, M^{-1} cm^{-1}):** 259 (34,740), 306 (25,330). **MS m/z (%):** 278.57 [M]. **^{1}H NMR (400 MHz, DMSO-d_6) δ/ppm:** 8.74 (2H, d, $J = 8.0$ Hz, $H_{2'',6''}$), 7.93 (2H, d, $J = 7.6$ Hz, $H_{3'5'}$), 7.77 (1H, s, H_6), 7.42 (3H, t, $^3J_1 = 8.0$ Hz, $^3J_2 = 8.0$ Hz, $H_{3'',4'',5''}$), 7.21–7.10 (2H, m, $H_{2',6'}$), 2.37 (3H, s, pyrazole-CH_3). **^{13}C NMR (100 MHz, DMSO-d_6) δ/ppm:** 165.56 (C=O, $C_{quat.}$), 147.83 (C_3, $C_{quat.}$), 143.40 (C_6,-CH), 140.32 ($C_{1''}$,$C_{quat.}$), 134.98 ($C_{2',6'}$, -CH), 133.56 ($C_{4'}$, $C_{quat.}$), 131.08 ($C_{1'}$, $C_{quat.}$), 128.90 ($C_{3'',5''}$, -CH), 128.50 ($C_{3',5'}$, -CH), 128.00 ($C_{4''}$, -CH), 126.23 (C_4, $C_{quat.}$), 118.57 ($C_{2'',6''}$, -CH), 15.26 (-CH_3, pyrazole). [**Total signal observed = 13:** signal of C = 6 (pyrazole-C = 3, phenyl ring-C = 3), signal of CH and CH3 = 7 (substituted pyarazole-CH = 1, phenyl ring-CH = 5, pyrazole-CH_3 = 1]. **FT-IR (KBr): (cm^{-1}):** 3078 $\nu_{(\text{=C-H})\text{ar}}$ (w), 1674 $\nu_{(\text{-N-C=O})}$, 1589 $\nu_{(\text{C=N})}$ (s), 1488 $\nu_{(\text{C=C})\text{conjugated alkenes}}$ (m), 1365–1411 $\nu_{(\text{C-H})\text{banding}}$ (m), 1311 $\nu_{(\text{C-N})}$, 1149 $\nu_{(\text{C-C})\text{alkanes}}$ (s), 756 $\nu_{(\text{Ar-H})2\text{ adjacent hydrogen}}$ (s).

2.3.5. Structural characterization of (E)-4-(4-bromobenzylidene)-5-methyl-2-phenyl-2,4-dihydro-3H-pyrazol-3-one (L^5)

This ligand (L^5) was prepared through the addition of 2-phenyl-5-methyl pyrazole-3-one (1a) (522 mg, 3 mmol) and p-bromo benzaldehyde (2e) (555 mg, 3 mmol) and reflux for 5–6 h in presences of catalytic amount AcOH and EtOH solution as described in general process. **Colour:** orange powder, **Yield:** 81%, **mol. wt.:** 341.21 g/mol, **m.p.:** 130 °C; **Anal. Calc. (%) For $C_{17}H_{13}BrN_2O$:** C, 59.84; H, 3.84; N, 8.21. **Found (%):** C, 59.39; H, 3.75; N, 8.34. **UV-vis: λ(nm) (ε, M^{-1} cm^{-1}):** 256 (34,400), 364 (15,340). **MS m/z (%):** 341.17 [M]. **^{1}H NMR (400 MHz, DMSO-d_6) δ/ppm:** 8.73 (2H, d, $J = 8.0$ Hz, $H_{2'',6''}$), 7.93 (2H, d, $J = 7.6$ Hz, $H_{3',5'}$), 7.76 (1H, s, H_6), 7.42 (3H, t, $^3J_1 = 8.4$ Hz, $^3J_2 = 8.4$ Hz, $H_{3'',4'',5''}$), 7.21–7.12 (2H, m, $H_{2',6'}$), 2.35 (3H, s, pyrazole-CH_3). **^{13}C NMR (100 MHz, DMSO-d_6) δ/ppm:** 165.56 (C=O, $C_{quat.}$), 147.84 (C_3, $C_{quat.}$), 143.43 (C_6,-CH), 140.39 ($C_{1''}$,$C_{quat.}$), 134.78 ($C_{2',6'}$, -CH), 131.96 ($C_{1'}$, Cquat.), 131.48 ($C_{3',5'}$, -CH), 128.90 ($C_{3'',5''}$, -CH), 128.00 ($C_{4''}$, -CH), 126.25 (C_4, $C_{quat.}$), 122.32 ($C_{4'}$, $C_{quat.}$), 118.56 ($C_{2'',6''}$, -CH), 15.00 (-CH_3, pyrazole). [**Total signal observed = 13:** signal of C = 6 (pyrazole-C = 3, phenyl ring-C = 3), signal of CH and CH_3 = 7 (substituted pyarazole-CH = 1, phenyl

ring-CH = 5, pyrazole-CH_3 = 1]. **FT-IR (KBr): (cm^{-1}):** 3070 ν(=C-H) ar (w), 1674 ν(-N-C=O), 1581 ν(C=N) (s), 1488 ν(C=C)$_{conjugated\ alkenes}$ (m), 1365–1411 ν(C-H)$_{banding}$ (m), 1311 ν(C-N), 1141 ν(C-C)$_{alkanes}$ (s), 756 ν(Ar-H)2 $_{adjacent\ hydrogen}$ (s).

2.3.6. Structural characterization of (E)-5-methyl-4-(4-nitrobenzylidene)-2-phenyl-2,4-dihydro-3H-pyrazol-3-one (L^6)

This ligand (L^6) was prepared through the addition of 2-phenyl-pyrazole-3-one (1a) (522 mg, 3 mmol) and *p*-nitro benzaldehyde (2f) (453 mg, 3 mmol) and reflux for 5–6 h in presences of catalytic amount AcOH and EtOH solution as described in general process. **Colour:** orange powder, **Yield:** 82%, **mol. wt.:** 307.31 g/mol, **m.p.:** 138 °C; **Anal. Calc. (%) For $C_{17}H_{13}N_3O_3$**: C, 66.44; H, 4.26; N, 13.67. **Found (%):** C, 66.39; H, 4.15; N, 13.64. **UV-vis: λ(nm) (ε, M^{-1} cm^{-1}):** 256 (34,400), 364 (15,340). **MS m/z (%):** 307.88 [M]. **^{1}H NMR (400 MHz, DMSO-d_6) δ/ppm:** 8.74 (2H, d, J = 11.6 Hz, $H_{2'',6''}$), 7.93 (2H, d, J = 6.0 Hz, $H_{3',5'}$), 7.76 (1H, s, H_6), 7.42 (3H, t, $^3J_1$ = 7.2 Hz, $^3J_2$ = 9.6 Hz, $H_{3'',4'',5''}$), 7.21–7.11 (2H, m, $H_{2',6'}$), 2.36 (3H, pyrazole-CH_3). **^{13}C NMR (100 MHz, DMSO-d_6) δ/ppm:** 165.47 (C=O, $C_{quat.}$), 147.80 (C_3, $C_{quat.}$), 147.13 ($C_{4'}$,-$C_{quat.}$), 143.49 (C_6,-CH), 140.38 ($C_{1''}$, -CH), 139.00 ($C_{1'}$, $C_{quat.}$), 132.28 ($C_{2',6'}$, -CH), 128.92 ($C_{3'',5''}$, -CH), 128.00 ($C_{4''}$, -CH), 126.27 (C_4, $C_{quat.}$), 123.83 ($C_{3',5'}$, $C_{quat.}$), 118.50 ($C_{2'',6''}$, -CH), 15.08 (-CH_3, pyrazole). [**Total signal observed = 13:** signal of C = 6 (pyrazole-C = 3, phenyl ring-C = 3), signal of CH and CH_3 = 7 (substituted pyarazole-CH = 1, phenyl ring-CH = 5, pyrazole-CH_3 = 1]. **FT-IR (KBr): (cm^{-1}):** 3050 $\nu_{(=C-H)ar}$ (w), 1681 $\nu_{(-N-C=O)}$, 1589 $\nu_{(C=N)}$ (s), 1488–1512 $\nu_{(C=C)conjugated\ alkenes}$ (m), 1342–1421 $\nu_{(C-H)banding}$ (m), 1303 $\nu_{(C-N)}$, 1110–1141 $\nu_{(C-C)alkanes}$ (s), 748 $\nu_{(Ar-H)2\ adjacent\ hydrogen}$ (s).

2.4. General synthesis of cycloplatinated(II) chloro bridge dimer [Pt(L^6)Cl]$_2$

Synthesis of the platinum(II) dichloro-bridged dimers was carried out using a modified method of Lewis [14,15]. To the solution of 2-phenyl-5-methyl pyrazole-3-one derivative ligands (L^1–L^6) (58.6 mg, 0.4 mmol) and K_2PtCl_4 (83 mg, 0.2 mmol) in ethoxyethanol, stirred vigorously under nitrogen (N_2) atm. and refluxed at 100 °C for 24–48 h. The reaction mixture was allowed to cool at room temperature. The obtained precipitate (chloro-bridged Pt(II) dimer) was washed with water (20 mL) and dried at 50 °C under vacuum. The crude product was used for next step without purification. The characterization data of dimer are as follows.

Colour: brown powder, **Yield:** 37%, **mol.wt.:** 1073.67 g/mol, **m.p.:** >300 °C; **Anal. Calc. (%) For $C_{34}H_{24}Cl_2N_6O_6Pt_2$. Conductance:** 22 $\Omega^{-1}cm^2mol^{-1}$. **^{1}H NMR (400 MHz, DMSO-d_6) δ/ppm:** 7.78–7.20 (16H, m, Ar-H), 6.10 (2H, s, $H_{6,6}$), 1.28 (6H, s, pyrazole-CH_3). **^{13}C NMR (100 MHz, DMSO-d_6) δ/ppm:** 169.50 (C=O, C_5), 152.81 (C_3, $C_{quat.}$), 147.14 ($C_{4'}$, C_{quat}), 142.68 (C_6, -CH), 141.82 ($C_{1''}$, $C_{quat.}$), 139.00 ($C_{1'}$, $C_{quat.}$), 132.23 ($C_{2',6'}$, -CH), 128.96 ($C_{3''}$, -CH.), 128.00 ($C_{5''}$, -CH), 128.00 ($C_{5''}$, -CH), 124.37 ($C_{4''}$, -CH), 123.82 ($C_{3',5'}$, -CH), 121.65 ($C_{2''}$,-CH.), 120.00 ($C_{6''}$, Cquat), 116.53 (C_4, $C_{quat.}$), 13.95 (CH_3, pyrazole). [**Total signal observed = 15:** signal of C = 7 (pyrazole-C = 3, phenyl ring-C = 4), signal of CH and CH_3 = 8 (pyrazole-CH = 1, phenyl ring-CH = 6, pyrazole-CH_3 = 1].

2.5. Preparation of cycloplatinum(II) complexes (I-VI)

The crude product (chloro-bridged Pt(II) dimer) was treated with 3 molar equivalent acetyl acetone in the presence of 10 equiv. of K_2CO_3 in 2-ethoxyethanol solvent at 80–90 °C under nitrogen (N_2) atmosphere for 24–48 h. The mixture was poured into water for extraction through separating funnel using solvent dichloromethane (CH_2Cl_2). The organic extracts were washed with water and dried over anhydrous sodium sulphate. After the solvent was completely evaporated, than the obtained residue was purified by column chromatography on silica gel with dichloromethane/petroleum ether (1:1) system as the eluent to obtained pure product. The proposed reaction mechanism for the synthesis of cyclometalated heteroleptic platinum(II) complexes (I-VI) are represented in Scheme 2. The ^{1}H NMR and ^{13}C NMR spectra of platinum(II) complexes are shown in supplementary material 1 and 2, respectively.

2.5.1. Synthesis of [(L^1)Pt(acac)]-I

It was prepared using [(L^1)PtCl]$_2$ dimer and acetyl acetone, according to the general procedure. **Colour:** brown powder, **Yield:** 67%, **mol. wt.:** 569.52 g/mol, **m.p.** >300 °C; **Anal. Calc. (%) For $C_{23}H_{22}N_2O_3Pt$:** C, 48.51; H, 3.89; N, 4.92; Pt, 34.25. **Found (%):** C, 48.30; H, 3.60; N, 4.67; Pt, 34.20. **Molar conductivity (Λ_m):** 21 $\Omega^{-1}cm^2mol^{-1}$. **UV-vis: λ (nm) (ε, M^{-1} cm^{-1}):** 308 (35,330), 360 (17,040). **^{1}H NMR (400 MHz, DMSO-d_6) δ/ppm:** 7.58–7.50 (9H, m, Ar-$H_{2',3',5',6',6,2'',3'',4'',5''}$), 6.57 (1H, s, $H_{3'''}$), 2.57 (3H, s, acac-$CH_{3\ 1'''}$), 1.66 (3H, s, acac-$CH_{3\ 5'''}$), 1.27 (3H, s, pyrazole-CH_3), 0.90 (3H, s, phenylring-CH_3). **^{13}C NMR (100 MHz, DMSO-d_6) δ/ppm:** 191.53 (C=O, $C_{quat.}$), 181.96 (C-O, $C_{4'''}$), 169.51 (C=O, C_5), 152.83 (C_3, $C_{quat.}$) 142.60 (C_6, -CH), 141.85 ($C_{1''}$, $C_{quat.}$), 137.63 ($C_{4'}$, $C_{quat.}$), 134.42 ($C_{2',6'}$, -CH), 129.93 ($C_{1'}$, $C_{quat.}$), 128.90 ($C_{3',5'}$, CH), 128.18 ($C_{3''}$, -CH), 128.00 ($C_{5''}$, -CH), 124.34 ($C_{4''}$, -CH), 121.60 ($C_{2''}$, -CH), 120.00 ($C_{6''}$,$C_{quat.}$), 116.72 (C4, $C_{quat.}$), 81.36 ($C_{3'''}$, -CH), 24.41 ($C_{5'''}$, -CH_3), 21.39 (-CH_3 aromatic), 16.09 (CH_3, $C_{1'''}$), 13.90 (CH_3, pyrazole). [**Total signal observed = 21:** signal of C = 9 (acetyl acetone-C = 2, pyrazole-C = 3, phenyl ring-C = 4), signal of CH and CH_3 = 12 (acetyl acetone-CH = 1, pyrazole-CH = 1, phenyl ring-CH = 6, acetyl acetone-CH_3 = 2, pyrazole-CH_3 = 1, phenyl ring-CH_3 = 1]. **FT-IR (KBr): (cm^{-1}):** 3105 $\nu_{(=C-H)ar}$ (w), 1558 $\nu_{(C=N)}$, $\nu_{(C=O)}$, 1419 $\nu_{(C=C)conjugated\ alkenes}$ (m), 1365 $\nu_{(C-H)banding}$ (m), 1018 $\nu_{(C-N)}$, 1265 $\nu_{(C-C)alkanes}$ (s), 609 $\nu_{(Pt-N)}$, 532 $\nu_{(Pt-O)}$.

2.5.2. Synthesis of [(L^2)Pt(acac)]-II

It was prepared using [(L^2)PtCl]$_2$ dimer and acetyl acetone, according to the general procedure. **Colour:** brown powder, **Yield:** 62%, **mol. wt.:** 585.52 g/mol, **m.p.** >300 °C; **Anal. Calc. (%) For $C_{23}H_{22}N_2O_4Pt$:** C, 47.18; H, 3.79; N, 4.78; Pt, 33.32. **Found (%):** C, 47.70; H, 3.62; N, 4.60; Pt, 33.37. **Molar conductivity (Λ_m):** 20 $\Omega^{-1}cm^2mol^{-1}$. **UV-vis: λ(nm) (ε, M^{-1} cm^{-1}):** 294.50 (25,210), 357 (6920). **^{1}H NMR (400 MHz, DMSO-d_6) δ/ppm:** 7.83–7.24 (9H, m, Ar-$H_{3',5',2',6',6,2'',3'',4'',5''}$), 6.04 (1H, s, $H_{3'''}$), 2.33 (3H, s, phenylring-OCH_3), 1.79 (3H, s, acac-$CH_{3\ 1'''}$), 0.99 (3H, s, acac-$CH_{3\ 5'''}$), 0.59 (3H, s, pyrazole-CH_3). **^{13}C NMR (100 MHz, DMSO-d_6) δ/ppm:** 191.52 (C=O, $C_{2'''}$), 181.90 (-C-O, $C_{4'''}$), 169.53 (C=O, C_5), 159.80 ($C_{4'}$, $C_{quat.}$), 152.86 (C_3, $C_{quat.}$), 142.65 (C_6, -CH), 141.83 ($C_{1''}$, $C_{quat.}$), 130.22 ($C_{2',6'}$, -CH), 128.90 ($C_{3''}$, -CH.), 128.50 ($C_{5''}$, -CH), 125.28 ($C_{1'}$, $C_{quat.}$), 124.30 ($C_{4''}$, -CH), 121.64 ($C_{2''}$, -CH), 120.06 ($C_{6''}$, $C_{quat.}$), 116.70 (C_4, $C_{quat.}$), 114.20 ($C_{3',5'}$, -CH), 81.32 ($C_{3'''}$, -CH), 55.81 (-OCH_3, aromatic), 24.40 ($C_{5'''}$, -CH_3), 16.09 (CH_3, $C_{1'''}$), 13.90 (CH_3, pyrazole). [**Total signal observed = 21:** signal of C = 9 (acetyl acetone-C = 2, pyrazole-C = 3, phenyl ring-C = 4), signal of CH and CH_3 = 12 (acetyl acetone-CH = 1, pyrazole-CH = 1, phenyl ring-CH = 6, acetyl acetone-CH_3 = 2, pyrazole-CH_3 = 1, phenyl ring-OCH_3 = 1]. **FT-IR (KBr): (cm^{-1}):** 3103 $\nu_{(=C-H)ar}$ (w), 1566 $\nu_{(C=N)}$, $\nu_{(C=O)}$, 1404 $\nu_{(C=C)conjugated\ alkenes}$ (m), 1360 $\nu_{(C-H)banding}$ (m), 1010 $\nu_{(C-N)}$, 1260 $\nu_{(C-C)alkanes}$ (s), 555 $\nu_{(Pt-N)}$, 509 $\nu_{(Pt-O)}$.

2.5.3. Synthesis of [(L^3)Pt(acac)]-III

It was prepared using [(L^3)PtCl]$_2$ dimer and acetyl acetone, according to the general procedure. **Colour:** brown powder, **Yield:** 65%, **mol. wt.:** 571.50 g/mol, **m.p.** >300 °C; **Anal. Calc. (%) For $C_{22}H_{20}N_2O_4Pt$:** C, 46.24; H, 3.53; N, 4.90; Pt, 34.14. **Found (%):** C, 46.27; H, 3.52; N, 4.70; Pt, 34.37. **Molar conductivity (Λ_m):**

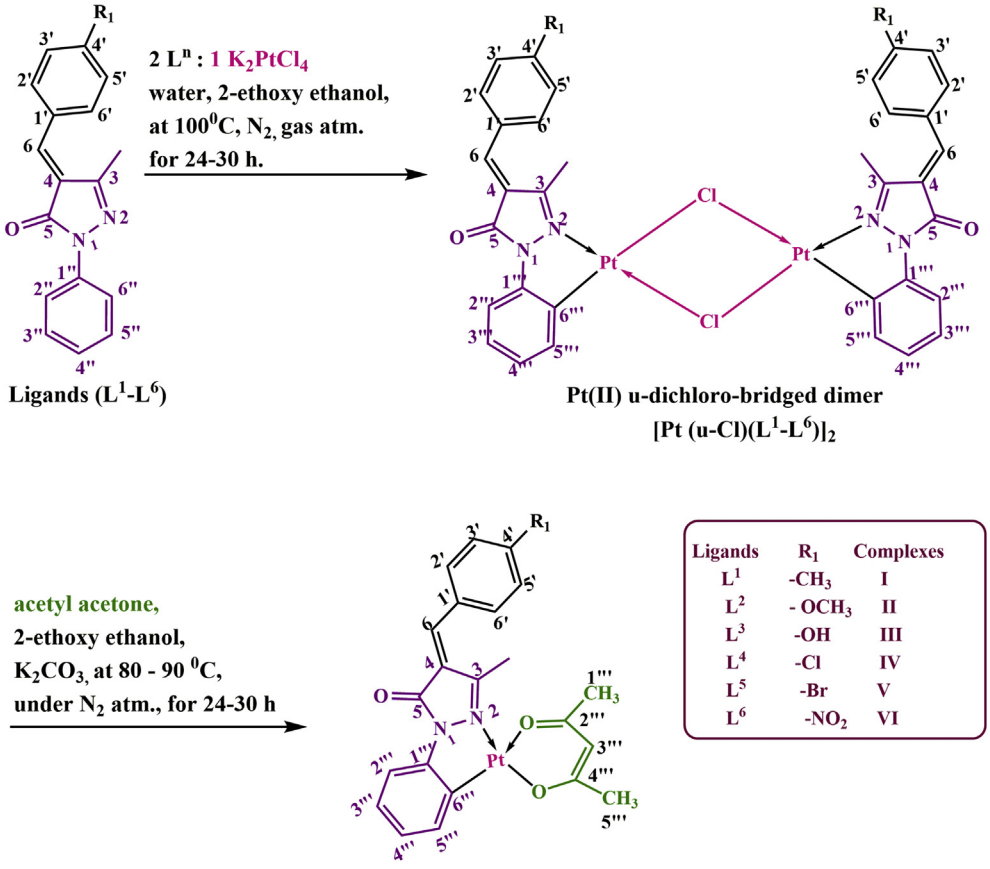

Scheme 2. Synthesis of the organometallic platinum(II) complexes **(I-VI).**

22 $\Omega^{-1}cm^2mol^{-1}$. **UV-vis: λ(nm) (ε, M^{-1} cm^{-1}):** 294.50 (25,210), 357 (6920). **^{1}H NMR (400 MHz, DMSO-d_6) δ/ppm:** 10.12 (1H, s, phenyl ring-OH), 7.78–7.20 (9H, m, Ar-$H_{2',3',5',6',2'',3'',4'',5''}$), 6.19 (1H, s, $H_{3'''}$), 1.97 (3H, s, acac-$CH_{3\ 1'''}$), 1.26 (3H, s, acac-$CH_{3\ 5'''}$), 0.89 (3H, s, pyrazole-CH_3). **^{13}C NMR (100 MHz, DMSO-d_6) δ/ppm:** 191.50 (C=O, $C_{2'''}$), 181.92 (-C-O, $C_{4'''}$), 169.52 (C=O, C_5), 157.73 ($C_{4'}$, $C_{quat.}$), 152.81 (C_3, $C_{quat.}$), 142.64 (C_6, -CH), 141.80 ($C_{1''}$, $C_{quat.}$), 130.62 ($C_{2',6'}$, -CH), 129.90 ($C_{3''}$, -CH.), 128.90 ($C_{5''}$, -CH), 125.58 ($C_{1'}$, $C_{quat.}$), 124.30 ($C_{4''}$, -CH), 121.62 ($C_{2''}$, -CH), 120.06 ($C_{6''}$, $C_{quat.}$), 116.74 (C_4, $C_{quat.}$), 115.80 ($C_{3',5'}$, -CH), 81.36 ($C_{3'''}$, -CH), 24.42 ($C_{5'''}$, -CH_3), 16.08 (CH_3, $C_{1'''}$), 13.96 (CH_3, pyrazole). [**Total signal observed = 20:** signal of C = 9 (acetyl acetone-C = 2, pyrazole-C = 3, phenyl ring-C = 4), signal of CH and CH_3 = 11 (acetyl acetone-CH = 1, pyrazole-CH = 1, phenyl ring-CH = 6, acetyl acetone-CH_3 = 2, pyrazole-CH_3 = 1]. **FT-IR (KBr): (cm^{-1}):** 3340 $\nu_{(O-H)}$, 3105 $\nu_{(=C-H)ar}$ (w), 1558 $\nu_{(C=N)}$, $\nu_{(C=O)}$, 1404 $\nu_{(C=C)conjugated\ alkenes}$ (m), 1365 $\nu_{(C-H)banding}$ (m), 1018 $\nu_{(C-N)}$, 1265 $\nu_{(C-C)alkanes}$ (s), 532 $\nu_{(Pt-N)}$, 509 $\nu_{(Pt-O)}$.

2.5.4. Synthesis of [(L^4)Pt(acac)]-IV

It was prepared using [(L^4)PtCl]$_2$ dimer and acetyl acetone, according to the general procedure. **Colour:** brown powder, **Yield:** 60%, **mol. wt.:** 589.94 g/mol, **m.p.** >300 °C; **Anal. Calc. (%) For $C_{22}H_{19}ClN_2O_3Pt$:** C, 44.79; H, 3.25; N, 4.75; Pt, 33.07. **Found (%):** C, 44.77; H, 3.42; N, 4.70; Pt, 33.17. **Molar conductivity (Λ_m):** 24 $\Omega^{-1}cm^2mol^{-1}$. **UV-vis: λ(nm) (ε, M^{-1} cm^{-1}):** 293 (27,030), 354 (8000). **^{1}H NMR (400 MHz, DMSO-d_6) δ/ppm:** 8.86–7.56 (9H, m, Ar-$H_{2',3',5',6',6,2'',3'',4'',5''}$), 6.18 (1H, s, $H_{3'''}$), 2.27 (3H, s, acac-$CH_{3\ 1'''}$), 1.68 (3H, s, acac-$CH_{3\ 5'''}$), 1.06 (3H, s, pyrazole-CH_3). **^{13}C NMR (100 MHz, DMSO-d_6) δ/ppm:** 191.52 (C=O, $C_{2'''}$), 181.94 (-C-O, $C_{4'''}$), 169.54 (C=O, C_5), 152.80 (C_3, $C_{quat.}$), 142.62 (C_6, -CH), 141.82 ($C_{1''}$, $C_{quat.}$), 134.92 ($C_{2',6'}$, -CH), 133.52 ($C_{4'}$, -CH.), 131.00 ($C_{1'}$, $C_{quat.}$), 128.98 ($C_{3''}$, -CH), 128.70 ($C_{3',5'}$, -CH), 128.05 ($C_{5''}$, -CH), 124.30 ($C_{4''}$, -CH), 121.60 ($C_{2''}$, -CH), 120.00 ($C_{6''}$, $C_{quat.}$), 116.70 (C_4, $C_{quat.}$), 81.34 ($C_{3'''}$, -CH), 24.49 (CH_3, $C_{5'''}$), 16.06 (CH_3, $C_{1'''}$), 13.91 (-CH_3, pyrazole). [**Total signal observed = 20:** signal of C = 9 (acetyl acetone-C = 2, pyrazole-C = 3, phenyl ring-C = 4), signal of CH and CH_3 = 11 (acetyl acetone-CH = 1, pyrazole-CH = 1, phenyl ring-CH = 6, acetyl acetone-CH_3 = 2, pyrazole-CH_3 = 1]. **FT-IR (KBr): (cm^{-1}):** 3001 $\nu_{(=C-H)ar}$ (w), 1558 $\nu_{(C=N)}$, $\nu_{(C=O)}$, 1404 $\nu_{(C=C)conjugated\ alkenes}$ (m), 1360 $\nu_{(C-H)banding}$ (m), 1010 $\nu_{(C-N)}$, 1265 $\nu_{(C-C)alkanes}$ (s), 563 ν(Pt-N), 509 ν(Pt-O).

2.5.5. Synthesis of [(L^5)Pt(acac)]-V

It was prepared using [(L^5)PtCl]$_2$ dimer and acetyl acetone, according to the general procedure. **Colour:** brown powder, **Yield:** 67%, **mol. wt.:** 634.08 g/mol, **m.p.** >300 °C; **Anal. Calc. (%) For $C_{22}H_{19}BrN_2O_3Pt$:** C, 41.65; H, 3.02; N, 4.42; Pt, 30.75. **Found (%):** C, 41.77; H, 3.01; N, 4.40; Pt, 30.17. **Molar conductivity (Λ_m):** 19 $\Omega^{-1}cm^2mol^{-1}$. **UV-vis: λ(nm) (ε, M^{-1} cm^{-1}):** 298 (29,910), 370 (10,050). **^{1}H NMR (400 MHz, DMSO-d_6) δ/ppm:** 7.78–7.19 (9H, m, Ar-$H_{2',3',5',6',6,2'',3'',4'',5''}$), 6.21 (1H, s, $H_{3'''}$), 2.31 (3H, s, acac-$CH_{3\ 1'''}$), 1.66 (3H, s, acac-$CH_{3\ 5'''}$), 0.97 (3H, s, pyrazole-CH_3). **^{13}C NMR (100 MHz, DMSO-d_6) δ/ppm:** 191.52 (C=O, $C_{2'''}$), 181.94 (-C-O, $C_{4'''}$), 169.54 (C=O, C_5), 152.80 (C_3, $C_{quat.}$), 142.62 (C_6, -CH), 141.82 ($C_{1''}$, $C_{quat.}$), 134.72 ($C_{2',6'}$, -CH), 131.92 ($C_{1'}$, $C_{quat.}$), 131.50 ($C_{3',5'}$, -CH), 128.95 ($C_{3''}$, -CH), 128.00 ($C_{5''}$, -CH), 122.30 ($C_{4'}$, $C_{quat.}$), 124.30 ($C_{4''}$, -CH), 121.65 ($C_{2''}$, -CH), 120.00 ($C_{6''}$, $C_{quat.}$), 116.75 (C_4, $C_{quat.}$), 81.33 ($C_{3'''}$, -CH), 24.44 (CH_3, $C_{5'''}$), 16.04 (CH_3, $C_{1'''}$), 13.95 (-CH_3, pyrazole). [**Total signal observed = 20:** signal of C = 9 (acetyl acetone-C = 2, pyrazole-C = 3, phenyl ring-C = 4), signal of CH and CH_3 = 11

(acetyl acetone-CH = 1, pyrazole-CH = 1, phenyl ring-CH = 6, acetyl acetone-CH_3 = 2, pyrazole-CH_3 = 1]. **FT-IR (KBr): (cm^{-1}):** 3001 $\nu_{(=C-H)ar}$ (w), 1558–1650 $\nu_{(C=N)}$, $\nu_{(C=O)}$, 1404 $\nu_{(C=C)conjugated\ alkenes}$ (m), 1350 $\nu_{(C-H)banding}$ (m), 1018 $\nu_{(C-N)}$, 1260 $\nu_{(C-C)alkanes}$ (s), 640 $\nu_{(Pt-N)}$, 478 $\nu_{(Pt-O)}$.

2.5.6. Synthesis of [(L^6)Pt(acac)]-VI

It was prepared using [(L^6)PtCl]$_2$ dimer and acetyl acetone, according to the general procedure. **Colour:** brown powder, **Yield:** 69%, **mol. wt.:** 600.49 g/mol, **m.p.** >300 °C; **Anal. Calc. (%) For $C_{22}H_{19}N_3O_5Pt$:** C, 44.00; H, 3.19; N, 7.00; Pt, 32.49. **Found (%):** C, 44.07; H, 3.12; N, 7.01; Pt, 32.47. **Molar conductivity (Λ_m):** 18 $\Omega^{-1}cm^2mol^{-1}$. **UV-vis: λ(nm) (ε, M^{-1} cm^{-1}):** 298 (29,910), 370 (10,050). **^{1}H NMR (400 MHz, DMSO-d_6) δ/ppm:** 7.79–7.22 (9H, m, Ar-$H_{2',3',5',6',2'',3'',4'',5''}$), 6.20 (1H, s, $H_{3'''}$), 2.26 (3H, s, acac-$CH_{3\ 1'''}$), 1.67 (3H, s, acac-$CH_{3\ 5'''}$), 0.97 (3H, s, pyrazole-CH_3). **^{13}C NMR (100 MHz, DMSO-d_6) δ/ppm:** 191.59 (C=O, $C_{2'''}$), 181.96 (-C-O, $C_{4'''}$), 169.51 (C=O, C_5), 152.87 (C_3, Cquat.), 147.12 ($C_{4'}$, Cquat.), 142.61 (C_6, -CH), 141.84 ($C_{1''}$, Cquat.), 139.00 ($C_{1'}$, Cquat.), 132.22 ($C_{2',6'}$, -CH), 128.92 ($C_{3''}$, -CH), 123.80 ($C_{3',5'}$, -CH), 128.00 ($C_{5''}$, -CH), 124.31 ($C_{4''}$, -CH), 121.68 ($C_{2''}$, -CH), 120.00 ($C_{6''}$, Cquat.), 116.73 (C_4, Cquat.), 81.30 ($C_{3'''}$, -CH), 24.40 (CH_3, $C_{5'''}$), 16.03 (CH_3, $C_{1'''}$), 13.93 (-CH_3, pyrazole). [**Total signal observed = 20:** signal of C = 9 (acetyl acetone-C = 2, pyrazole-C = 3, phenyl ring-C = 4), signal of CH and CH_3 = 11 (acetyl acetone-CH = 1, pyrazole-CH = 1, phenyl ring-CH = 6, acetyl acetone-CH_3 = 2, pyrazole-CH3 = 1]. **FT-IR (KBr): (cm^{-1}):** 2993 $\nu_{(=C-H)ar}$ (w), 1558–1650 $\nu_{(C=N)}$, $\nu_{(C=O)}$, 1411 $\nu_{(C=C)conjugated\ alkenes}$ (m), 1350 $\nu_{(C-H)banding}$ (m), 1018 $\nu_{(C-N)}$, 1260 $\nu_{(C-C)alkanes}$ (s), 555 $\nu_{(Pt-N)}$, 501 $\nu_{(Pt-O)}$.

2.6. Biological application of the synthesized compounds

2.6.1. In vitro antibacterial activity

All of the newly synthesized Pt(II) complexes (I-VI) were screened for their antibacterial activity using *Staphylococcus aureus, Bacillus subtilis, Serratia marcescens, Pseudomonas aeruginosa and Escherichia coli* micro-organisms. The broth dilution technique has been used to determine the bactericidal effect by minimum inhibitory concentration (MIC) in terms of μM. MIC, lowest concentration that prevents the microbial growth incubated at 37 ± 1 °C for 24 h. MIC was determined in liquid media containing 0.2–3500 μM of the test compound. A preculture of bacteria was grown in Luria broth overnight at 37 °C. First culture was used as a control to examine normal growth and second culture 20 μL of the bacteria and compound at the desired concentration were added to monitor bacterial growth by measuring turbidity of the culture after 18 h. If a certain concentration of a compound inhibit bacterial growth, half of the concentration of the compound was tested. This procedure was carried out up to the concentration that inhibited the growth of bacteria. All equipment and culture media were sterilized.

2.6.2. In vitro cytotoxicity against brine shrimp lethality bioassay

For the determination of toxicity of bioactive compounds *in vitro* cytotoxicity technique was used. Brine shrimp (*Artemia cysts*) Lethality bioassay method given by Meyer et al. [16] accomplished with brine shrimp nauplii in artificial seawater (prepared with a commercial salt mixture in double distilled water) and using approximately 50 mg eggs in ordinary light. After 24 h, keeping constant volume 2.5 mL per vial accumulate 1 mL of seawater and 10 shrimps (collected nauplii using a pipette) in each vial, then add a sample solution (from 10 mg in 10 mL) in it to make final concentrations of solution 2, 4, 8, 12, 16 and 20 mg mL^{-1} (triplicate sets 18 vials) along with control (3 vials) having only DMSO with same amount finally volume adjust by seawater. After 24 h, counted the number of viability of nauplii (observing several seconds if nauplii did not exhibit any internal or external movement considered nauplii dead). Data were analysed by the log concentration of sample vs percentage mortality of nauplii that gives LC_{50} values. All data has been collected from three independent experiments and the LC50 determined using OriginPro 8 software.

2.6.3. In vitro cellular level cytotoxicity against S. Pombe cells

Eukaryotic *Schizosaccharomyces pombe* was an important organism for the study of effects of the metal complexes at cellular level (cytotoxicity) to the DNA damage (genotoxicity). *S. pombe* were grown in liquid yeast extract media in 150 mL Erlenmeyer flask containing 50 mL of yeast extract media. To acquire the enough growth of *S. pombe*, flask was incubated at 30 °C on shaker at 150 rpm (24–30 h). Then the cell culture was treated with synthesized ligands and complexes at different concentrations (20, 40, 60, 80, 100 μM), which were dissolve in DMSO took as a control and further allowed to growth for 16–18 h. Next day, centrifuge the treated and control cells at 12,000 rpm for 10 min to remove the media and wash the cells with phosphate buffer saline (PBS) thrice. Resuspend the cells in 500 μL of PBS. Take the equal volume of cells suspension and 0.4% trypan blue dye in PBS to incubate for 5 min at room temperature. Cells-dye mixture were put on glass slide and cells were observed in a compound microscope (40X). Dead cells were permitting trypan blue dye to appear the blue whereas live cells resisted the entry of dye seen in colourless. Percentage viability were count in triplicate where number of dead cells and number of live cells were counted in three microscopic fields and calculated average percentage of live cells [17].

2.6.4. DNA interaction studies

2.6.4.1. (a) Electronic absorption titration spectroscopy. Binding mode and interaction strength of DNA with metal complexes have been examined effectively by electronic absorption spectra (UV–Vis absorbance titration) using Herring Sperm DNA (HS-DNA) with ε = 12,858 dm^3 mol^{-1} cm^{-1} in phosphate buffer solution (pH 7.2). The stock solutions of the complexes were prepared in DMSO. The absorption titration has been performed by the concentration of complex keeping constant (20 μM) and continuous adding the volume of DNA (100 μL), and incubated for 10 min at room temperature. By using absorption spectral titration data K_b value have been determined from the ratio of the slope to intercept from plot of [DNA]/(ε_a–ε_f) versus [DNA] [18–21].

2.6.4.2. (b) Viscosity measurements. An Ubbelohde viscometer maintained at a constant temperature of 27 ± 0.1 °C in a thermostatic jacket. It was used to measure the flow time of HS-DNA in phosphate buffer (pH 7.2) with a digital stopwatch. Flow time measurements of each compound were carried out three times to calculate average flow time. Data were presented as relative specific viscosity $((\eta/\eta_0)^{1/3})$ vs binding ratio ([Drug]/[DNA] [22], where η and η_0 is the viscosity of DNA in the presence of complex and viscosity of DNA alone, respectively. Viscosity values have been calculated from the observed flow time of DNA containing solutions ($t > 100$ s), corrected for the flow time of buffer alone (t_0), $\eta \propto t - t_0$ [23].

2.6.4.3. (c) Fluorescence quenching analysis. Emission intensity measurements of ethidium bromide (EB = 3,8-diamino-5-ethyl-6-phenylphenanthridinium bromide) with free HS-DNA in the absence and presence of Pt(II) complexes were performed in phosphate buffer. The HS-DNA solution was up to the value of r = 3.33 ([DNA]/[Complex]) of pre-treated EB–DNA mixture ([EB] = 33.3 μM, [DNA] = 10 μM) at ambient temperature and incubate for 10 min before measurement. The emission intensity

was recorded in the range of 500–800 nm. The emission intensities at 610 nm (λ_{max}) were obtained through excitation at 510 nm and slit wavelength 1.45 nm in the FluoroMax-4, HORIBA (Scientific) spectrofluorometer. The changes in fluorescence intensities of ethidium bromide and ethidium bromide bound to DNA were measured with respect to different concentration of the complex. The ethidium bromide has less-emission intensity in phosphate buffer solution 7.2 pH due to fluorescence quenching of free ethidium bromide by the solvent molecules. In the presence of DNA, EB exhibits higher intensity due to its partial intercalative binding mode to DNA. Fluorescence quenching of an EB-DNA can arise owing to inner-filter effect. The mechanism of quenching is found from the emission intensity of EB. In our study, inner filter effect was corrected with the following equation in this literature [24,25].

To examine the fluorescence quenching mechanism, the Stern–Volmer quenching constant (K_{sv}) was determined by equation (1): [26,27]

$$I^{\circ}/I = Ksv[Q] + 1 \quad (1)$$

where, I_0 and I are the emission intensity of EB-DNA in the absence and presence of quencher (complex), K_{sv} is the linear Stern-Volmer quenching constant obtained from the plot of I_0/I vs. [Q] and [Q] is concentration of quencher. To determine the strength of the interaction of complexes with DNA, the value of the associative binding constant (K_a) was calculated using the Scatchard equation (2): [28,29]

$$log\ I_{\circ} - I/I = \log Ka + nlog[Q] \quad (2)$$

where, I_0 and I are the fluorescence intensities of the EB-DNA in the absence and presence of different concentrations of complexes, respectively and n is the number of binding. The acting forces between drugs and biomacromolecules include hydrogen bonds, van der Waals forces, electrostatic attraction and hydrophobic interaction, etc. In order to estimate the interaction force of all compounds, the standard free energy changes (ΔG) for the binding process have been calculated using the Van't Hoff equation (3): [30]

$$\Delta G^{\circ} = -RTlnKa \quad (3)$$

where, T is the temperature (25 °C, 298 K here), K_a is associative binding constant and R is gas constant 8.314 $Jmol^{-1}\ K^{-1}$. The negative sign for ΔG° means that the binding process is spontaneous.

2.6.4.4. (d) Molecular docking study. Interaction between DNA and complexes at the molecular level were studied by advanced computational typical technique like molecular docking. The rigid molecular docking study has been executed using HEX 8.0 software to conclude the orientation of the Pt(II) complexes binding to DNA. The most stable configuration was selected as the input for investigation. Mole file of coordinates of metal complexes was prepared for optimized structure and were rehabilitated to.pdb format using CHIMERA 1.5.1 software. HS-DNA used in the experimental, the structure of the DNA of sequence (5′-d(CGCGAATTCGCG)-3′)$_2$ (PDB id: 1BNA, a familiar sequence used in oligodeoxynucleotide study) obtained from the Protein Data Bank (http://www.rcsb.org/pdb). All calculations were carried out on an Intel CORE i5, 2.20 GHz based machine running MS Windows 8.1 64 bit as the operating system. The by default parameters were used for the docking calculation with correlation type shape only, FFT mode at 3D level, grid dimension of 6 with receptor range 180 and ligand range 180 with twist range 360 and distance range 40 [31].

2.6.5. DNA nuclease study

Gel electrophoresis study was performed using pUC19 DNA with synthesized compounds. The samples were incubated for 0.5 h at 37°C. The samples were analysed by 1% agarose gel electrophoresis [Tris–acetate–ethylenediaminetetraacetic acid, (TAE) buffer, pH 8.0] for 3 h at 100 mV. The gel was stained with (0.5 mg mL^{-1}) ethidium bromide. The gels were viewed in an Alpha Innotech Corporation Gel doc system and photographed using a CCD camera. The cleavage efficiency of the compounds, the degree of DNA cleavage activity was measured by determining the ability of the complex to SC-DNA to OC-DNA equation describe in literature [32].

3. Results and discussion

3.1. UV-vis spectroscopy, molar conductivity measurements and magnetic moment

The geometry of the cyclometalated heteroleptic platinum(II) complexes has been confirmed using electronic spectral analysis. The cyclometalated platinum(II) complexes (I-VI) exhibit two intense bands, in the range of 294–308 nm and 354–370 nm due to charge transfer (CT) and DMSO-d_6 transitions, respectively [33,34]. Electronic spectral data of synthesized ligands (L^1-L^6) and complexes (I-VI) are represented in experimental section. The magnetic moments of Pt(II) complexes are zero B.M. and are consistent with low-spin $t_2g^6\ eg^2$ (d^8) configuration square planer geometry having dsp^2 hybridisation. All the cyclometalated Pt(II) complexes are diamagnetic in nature [35]. The molar conductivity (Λ_m) of platinum(II) complexes are observed in the range of 18–25 $\Omega^{-1}cm^2mol^{-1}$, which suggests the non-electrolytic nature of the complexes.

3.2. Fourier transform infrared spectroscopy (FT-IR)

FT-IR spectral data of synthesized ligands (L^1-L^6) and cyclometalated heteroleptic platinum(II) complexes (I-VI) are presented in experimental section. The peaks of ligands containing azomethine ν(C=N) group is observed in the range of 1514–1604 cm^{-1} and it is shifted to higher frequencies (1558–1650 cm^{-1}) in the complexation, showing the coordination of the heterocyclic nitrogen atoms (azomethine group) to platinum metal ion [36,37]. The bands $\nu C = C_{ar}$ of the compounds are observed in the of range 1488–1504 cm^{-1}. The $\nu C{-}H_{ar.}$ banding band of the free ligands are observed in the range of 1365–1411 cm^{-1} and it is shifted to lower frequency in the range of 1366-1350 cm^{-1} on complexation. The spectra of all the platinum(II) complexes show bands in the range of 532–640 cm^{-1}, 478-530 cm^{-1} and 416–430 cm^{-1}, due to (Pt-N), (Pt-O) and (Pt-C), respectively. In platinum(II) complexes (I-VI), the peak of acetylacetone group containing (>C=O) is observed in the range of 1650 cm^{-1}.

3.3. ^1H NMR spectroscopy

The ^1H NMR spectra of the 2-phenyl-5-methyl pyrazolone based ligands (L^1-L^6) and cyclometalated platinum(II) complexes (I-VI) have been obtained in solvent DMSO-d_6 and represented in supplementary material 1. The resultant physicochemical data of synthesized compounds are summarized in experimental section. In 2-phenyl-5-methyl pyrazolone based ligands (L^1-L^6), all the aromatic proton are observed in the range of ~δ 7.104–8.716 ppm and all aromatic proton of the cyclometalated platinum(II) complexes are appeared in the range of ~δ 7.585 to 7.501 ppm. Methoxy group of ligand (L^2) and complex (II) are appeared at about ~δ 2.344 and ~δ 2.338 ppm, respectively. Methyl (-CH_3) group of ligand (L^1) and complex (I) are observed at about ~δ 2.33 and ~δ 0.902 ppm,

respectively. All the cyclometalated platinum(II) complexes contain acetylacetone bidentate ligands. Therefore methyl group protons are obtained in range of ~δ 0.998–2.574 ppm. Hydroxy group of ligand (L^3) and complex (III) are observed proton peak at about ~δ 9.958 ppm and ~δ 10.120 ppm, respectively.

3.4. ^{13}C NMR spectroscopy

The ^{13}C NMR spectra of the synthesized 2-phenyl-5-methyl pyrazolone based aromatic ligands, cyclometalated heteroleptic platinum(II) complexes and μ-dichloro bridge complex (I) are shown in supplementary material 2 and data of these compounds are represented in experimental section. The peak of ligand (L^2) containing methoxy group and ligand (L^1) containing methyl group are appeared at 55.81 ppm and 21.34 ppm, respectively. These peaks are shifted to downfield in complex (II) and complex (I). The cyclometalated heteroleptic platinum(II) complexes (I-VI) containing acetylacetone bidentate ligands having > C=O peak observed in range of 181.90–191.52 ppm. The peak of phenyl ring carbon (-CH, $C_{6''}$) of free ligands (L^1-L^6) and phenyl ring carbon (-$C_{quat,}$ $C_{6''}$) of cyclometalated platinum(II) complexes are observed in the range of 118.50–118.57 ppm and 12.00–120.06 ppm, respectively. These observation suggest that the complexes exhibit downfield shift as compared to free ligands.

3.5. Mass spectrometry

The LC-MS spectrum and possible mass fragmentation pattern of complex (VI) are shown in Fig. 1. The mass spectra and mass fragmentation pattern of the synthesized ligands (L^1-L^6) are represented in supplementary material 3. Mass spectral data of the ligands are shown in experimental section. The mass spectrum of a synthesized platinum(II) complex (VI) shows a molecular ion peak at 600.62 *m/z* indicates that the absence of the chlorine atom in the complex. The peak at 501.27 *m/z* is due to 2-phenyl-5-methyl pyrazole-3-one derivative ligands attached to platinum metal ion with loss of acetylacetone moiety. The peak at 307.24 *m/z* corresponds to 2-phenyl pyeazole-3-one based ligands. The peaks at 174.37 *m/z* is obtained with loss of nitrobenzene ring in the presence of 2-phenyl-5-methyl pyrazole-3-one derivative ligand. The peak at 97.28 *m/z* is observed phenyl ring in the presence of 2-phenyl-5-methyl pyrazole-3-one derivative ligand.

3.6. Thermogravimetric analysis (TGA)

TGA shows the two steps of decomposition (supplementary material 4). The complex (VI) shows a no weight loss up to temperature 30–200 °C, indicating the absence of lattice and coordinate water molecule. In first step weight loss (16.48%) during 220–250 °C correspond to coordinated acetyl acetone bidentate ligand. In the second step, weight loss (51.17%) in between 260 and 430 °C correspond to 2-phenyl-5-methyl pyrazole-3-one derivative ligand. Platinum metallic (Pt) as a residue left behind at the end of TG curve (>800 °C) was used to calculate the metal content and was found in close proximity to the expected one.

3.7. Biological applications of synthesized compounds

3.7.1. In vitro antibacterial activity

The antimicrobial activity is carried out in terms of minimum inhibitory concentration (MIC) defined as the lowest concentration, which inhibits the growth of microorganism, referred by lack of turbidity in the tube. The result of this study are represented in Table 1. The IC_{50} values of the complexes and ligands are observed in range of 22–95 μM and 225–265 μM, respectively. The platinum(II) complexes (I-VI) exhibit higher antimicrobial activity than metal salt and 2-phenyl-5-methyl pyrazole-3-one based ligands (L^1-L^6) [38]. The *in vitro* antimicrobial bioassay of the metal complexes can be described on the basis of Tweedy's chelation theory [39]. Chelation decreases the polarity of metal ion due to partial

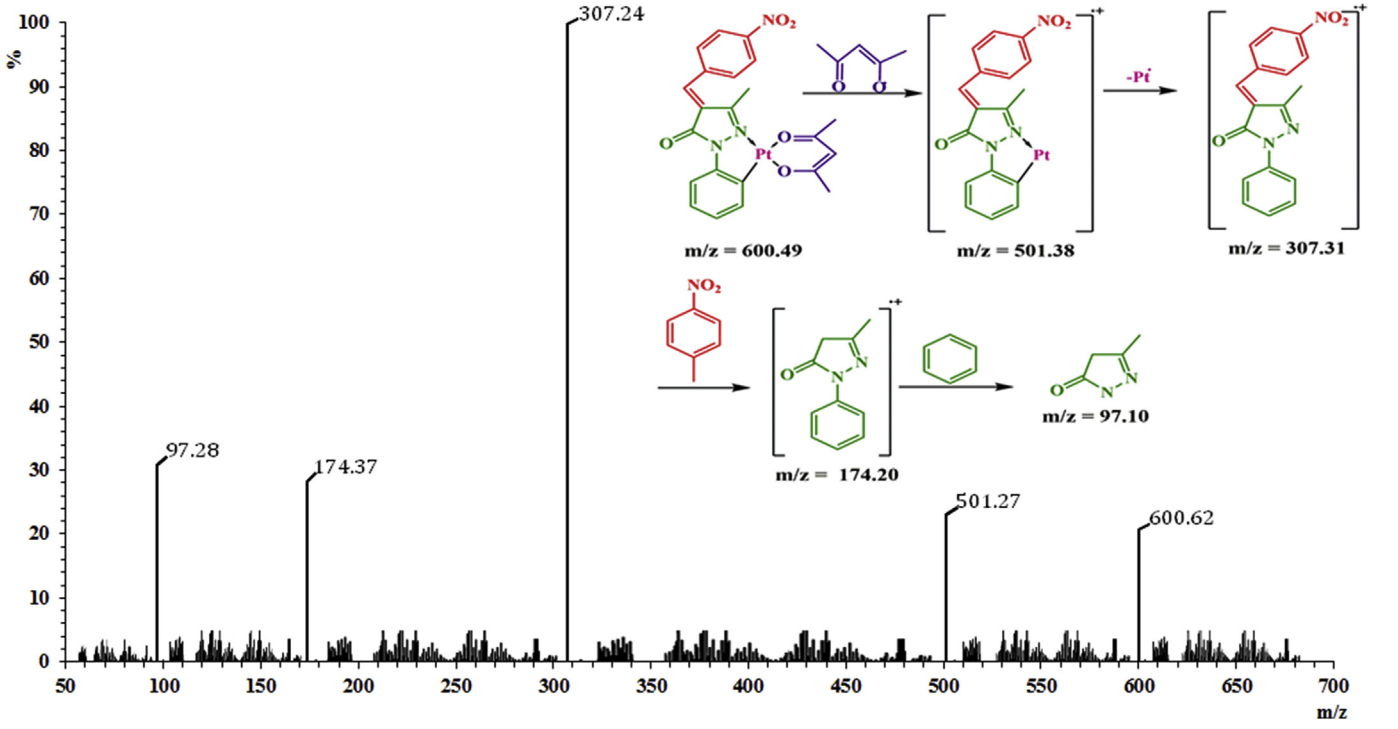

Fig. 1. LC-MS spectrum and fragmentation pattern of the synthesized organometallic platinum(II) complex (VI).

Table 1
The effects of inhibitory concentration (MIC, μM) values of the free ligands (L^1-L^6) and synthesized platinum(II) complexes (I-VI) against two Gram$^{(+ve)}$ and three Gram$^{(-ve)}$ microorganisms. Error bars represent the standard deviation of three independent ±5%.

Compounds	**Gram$^{(+ve)}$ bacteria**		**Gram$^{(-ve)}$ bacteria**		
	S. Aureus	*B. subtilis*	*S. marcescens*	*P. aeruginosa*	*E. coli*
K_2PtCl_4	2792 ± 1	2688 ± 2	2756 ± 1	2956 ± 1	3289 ± 1
L^1	248 ± 1	245 ± 1	240 ± 2	260 ± 2	265 ± 2
L^2	245 ± 2	240 ± 1	260 ± 1	236 ± 2	250 ± 2
L^3	228 ± 2	225 ± 2	230 ± 2	245 ± 2	255 ± 1
L^4	230 ± 2	227 ± 1	230 ± 2	240 ± 1	245 ± 1
L^5	232 ± 2	245 ± 1	250 ± 2	245 ± 1	250 ± 1
L^6	225 ± 2	245 ± 5	235 ± 1	240 ± 1	236 ± 5
I	89 ± 5	85 ± 1	90 ± 1	95 ± 3	80 ± 1
II	60 ± 2	70 ± 2	75 ± 1	75 ± 2	80 ± 2
III	35 ± 3	40 ± 1	45 ± 5	42 ± 5	40 ± 1
IV	50 ± 1	45 ± 2	42 ± 1	40 ± 2	60 ± 1
V	55 ± 1	39 ± 1	40 ± 3	60 ± 1	55 ± 2
VI	25 ± 2	30 ± 1	22 ± 2	35 ± 1	32 ± 1

sharing of its positive charge with donor groups and possible π-electron delocalization over the whole chelate ring. As a result lipophilic character of the central metal atom increases, approving its permeation through the lipid layer of the cell membrane and quickly attack the metal binding sites on enzymes of microorganism which inhibit the further growth of the organism [40].

3.7.2. *In vitro cytotoxicity against brine shrimp lethality bioassay*

All the synthesized 2-phenyl-5-methyl pyrazole-3-one based ligands (L^1-L^6) and cyclometalated platinum(II) complexes (I-VI) have been tested for *in vitro* brine shrimp lethality bioassay using Meyer et al. process [41]. The percentage mortality of brine shrimp nauplii has been determined from the number of dead nauplii. The LC_{50} value is calculated from the plot of log of concentration of samples against percentage of mortality of nauplii and data are represented in Table 2. It is concluded that the platinum(II) complexes show excellent toxicity as compared to corresponding ligands. The mortality rate of nauplii is found to increase with increasing concentration of compounds. The LC_{50} values of ligands and complexes are observed in the range of 52.44–99.97 μg/mL and 6.373–13.89 μg/mL, respectively. The LC_{50} values of cisplatin and transplatin are 3.133 and 14.45 μg/mL. The potency of the synthesized compounds are observed in order of cisplatin > VI > III > IV > V > II > I > transplatin > L^6 > L^3 > L^4 > L^5 > L^2 > L^1. *In vitro* cytotoxicity study is a basic one and additional studies are necessary to investigate its actual mechanism of cytotoxicity and its probable effects on cancer cell line.

Table 2
The Lethal Concentration (LC_{50}) values of cisplatin, transplatin and synthesized ligands (L^1-L^6) and Pt(II) complexes (I-VI) in μg/mL using *in vitro* cytotoxicity against brine shrimp lethality bioassay. Error bars represent the standard deviation of three replicates ±5%.

Compounds	Lethal Concentration (LC_{50}) in μg/mL
Ligand (L^1)	99.97 ± 1
Ligand (L^2)	90.26 ± 2
Ligand (L^3)	60.21 ± 5
Ligand (L^4)	68.91 ± 1
Ligand (L^5)	79.43 ± 1
Ligand (L^6)	52.44 ± 1
Cisplatin	3.133 ± 2
Transplatin	14.45 ± 2
Complex-I	13.89 ± 2
Complex-II	11.99 ± 5
Complex-III	6.45 ± 1
Complex-IV	9.168 ± 2
Complex-V	9.212 ± 1
Complex-VI	6.367 ± 2

3.7.3. *In vitro cellular level cytotoxicity against S. Pombe cells*

Cellular level *in vitro* cytotoxicity of the ligands and complexes have been tested by *S. pombe* cells. From the conclusion, cell death caused by toxicity of the compounds could be easily monitored by trypan blue dye as a staining. The potency has found to vary with the different type of functional group present and differ concentrations of the ligands and platinum(II) complexes. Complexes **III, IV**, **V** and **VI** (-OH, -Cl, -Br and $-NO_2$) are found to be excellent toxic as compared to other complexes (**I** and **II**), All the platinum(II) complexes (I-VI) are more toxic in nature as compared to 2-phenyl-5-methyl pyrazole-3-one based ligands (L^1-L^6). The *in vitro* cytotoxicity potency of the platinum(II) complexes is comparable to standard drug cisplatin and transplatin. After 17–20 h of the treatment, many of the *S. pombe* cells are destroyed due to toxic nature of the complexes. The cytotoxicity order of the synthesized compounds are Cisplatin > VI > IV > V > III > II > I > Transplatin > L^6 > L^4 > L^5 > L^3 > L^2 > L^1. The % viability data of the compounds are represented in Table 3.

3.7.4. *Structure-activity relationship (SAR)*

The results of the biological screening shown that the activity is widely affected by introducing different substituted benzyl ring on 2-phenyl-5-methyl pyrazole-3-one nucleus (Fig. 2). The methoxy group existing at 4th position on benzyl moiety (R_1 = -OCH_3) (complex-**II** and **III**) exhibits excellent antibacterial activity against two Gram positive bacteria i.e. *B. substiles* and *S. aureus*. The complexes **V** and **VI** containing R_1 = -NO_2 and −Br groups at 4th position on benzyl moiety, increase antibacterial activity against *B. substiles* and *S. marcescens*. The complex **I** exhibits the increasing antibacterial values (MIC) against *E. coli* bacteria due to presence of -CH_3 group. The complex **IV** having chloro (R_1 = -Cl) group at 4th position on benzyl moiety shows increasing anti-bacterial activity against Gram negative bacteria i.e. *S. marcescens* and *P. aeruginosa.* The presence of electron withdrawing functional groups in complexes such as complexes **III, IV, V** and **VI** exhibit superior antibacterial activity against Gram$^{(+ve)}$ and Gram$^{(-ve)}$ micro-organism as compared to other electron donating group in complexes **I** and **II**. The LC_{50} value and percentage viability values of the electron withdrawing functional group containing complexes **III**, **IV**, **V** and **VI** exhibit higher potency as compared to other electron releasing functional groups containing complexes **I** and **II**.

Table 3
The effect of compounds on % viability of *S. Pombe* cells at different concentrations (μM) with error uncertainty in the value ± 5%.

Concentration(μM)	20	40	60	80	100
Compounds	% Viability				
L^1	93 ± 1	90 ± 2	88 ± 2	85 ± 1	82 ± 1
L^2	88 ± 1	85 ± 2	84 ± 1	81 ± 1	78 ± 2
L^3	80 ± 1	77 ± 2	74 ± 1	71 ± 2	70 ± 2
L^4	78 ± 2	75 ± 2	73 ± 1	71 ± 1	70 ± 2
L^5	81 ± 2	80 ± 2	77 ± 3	76 ± 2	73 ± 2
L^6	72 ± 1	69 ± 1	67 ± 2	64 ± 2	63 ± 1
Cisplatin	59 ± 1	56 ± 1	49 ± 4	44 ± 2	37 ± 5
Transplatin	67 ± 1	57 ± 4	52 ± 5	48 ± 5	43 ± 1
I	65 ± 3	63 ± 1	60 ± 1	58 ± 3	55 ± 1
II	63 ± 5	60 ± 5	57 ± 2	53 ± 1	49 ± 3
III	61 ± 1	58 ± 2	51 ± 2	48 ± 2	42 ± 2
IV	58 ± 1	56 ± 1	49 ± 5	45 ± 1	40 ± 2
V	60 ± 2	57 ± 1	50 ± 1	47 ± 1	41 ± 1
VI	54 ± 2	52 ± 2	40 ± 1	39 ± 3	37 ± 1
DMSO	96 ± 2				
Untreated cell	98 ± 3				

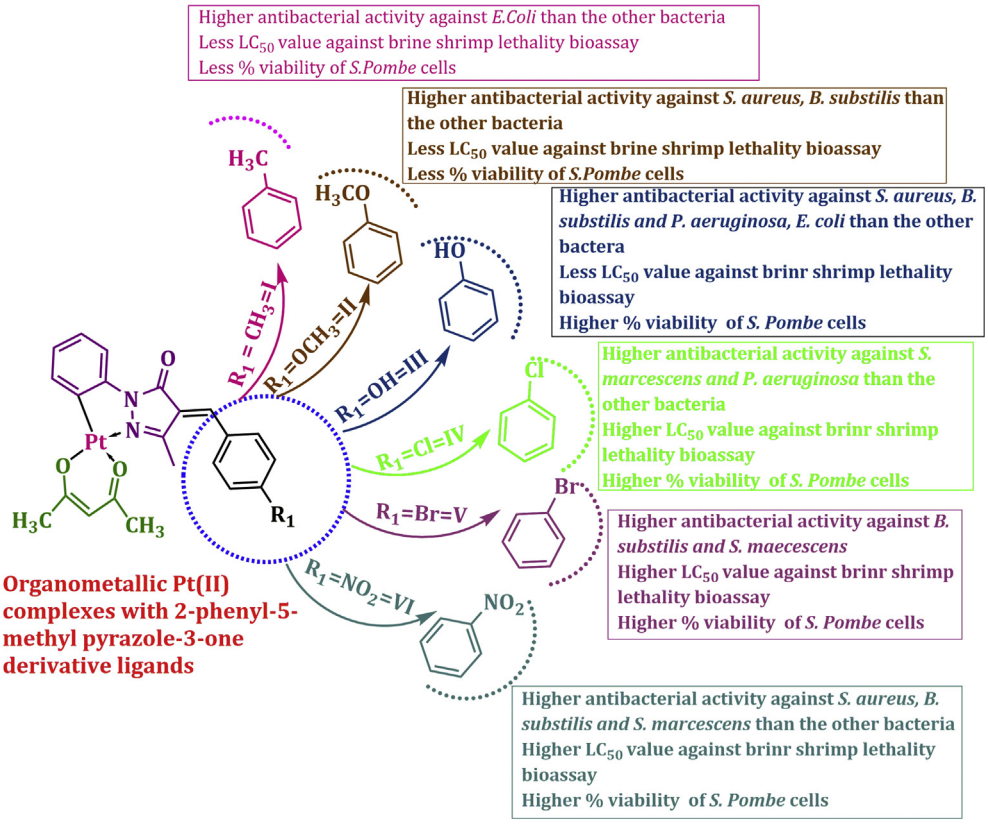

Fig. 2. Structure-activity relationship of complexes against antibacterial activity (MIC), *in vitro* cytotoxicity against brine shrimp lethality bioassay (LC_{50}) and cellular level cytotoxicity against *S. Pombe* cells (% viability).

3.7.5. DNA interaction studies

3.7.5.1. (a) Electronic absorption titration spectroscopy. Electronic absorption titration spectroscopy is most useful spectroscopic method for examine the interaction of substituted 2-phenyl-5-methyl pyrazole-3-one based ligands (L^1-L^6) and cyclometalated heteroleptic platinum(II) complexes with HS-DNA. A compounds interact with HS-DNA through intercalative mode of binding is a result of hypochromism and bathochromism [42]. The electronic absorption titration spectra of the ligand (L^6) and cyclometalated platinum(II) complex (VI) in the absence and presence of HS-DNA are represented in Fig. 3 and Fig. 4, respectively. The strong absorption bands of the ligands (L^1-L^6) and complexes (I-VI) are observed at about 254–380 nm [43]. The experimental obtained hypochromic effect in the intraligand transition band proposes that the compounds bind to HS-DNA via

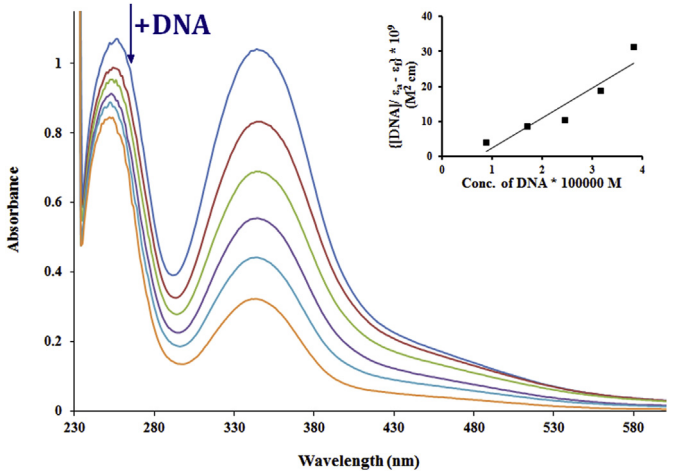

Fig. 3. Absorption spectra of ligand (L^6) (400 μM) in the absence and presence of increasing amounts of HS-DNA in phosphate buffer (Na_2HPO_4/NaH_2PO_4, pH = 7.2) solution, after incubation at room temperature for 10 min. The arrows show the absorbance changes upon the addition of the DNA concentrations. Insets: Linear plot of [DNA]/(ε_a-ε_f) vs. [DNA] for the titration of the ligand (L^6) with HS-DNA.

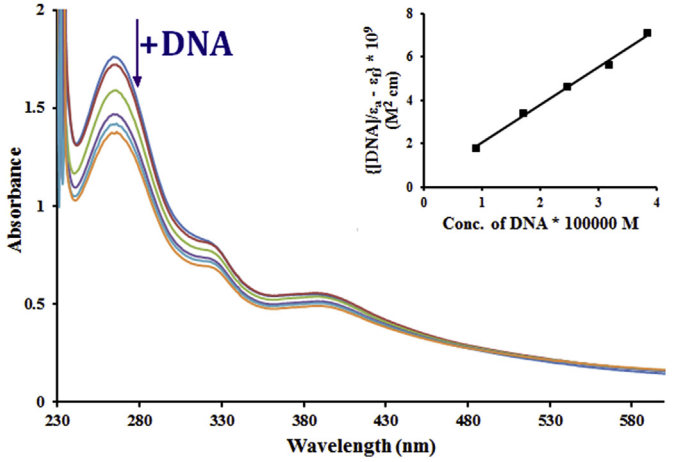

Fig. 4. Absorption spectra of Pt(II) complex (VI) (400 μM) in the absence and presence of increasing amounts of HS-DNA in phosphate buffer (Na_2HPO_4/NaH_2PO_4, pH = 7.2) solution, after incubation at room temperature for 10 min. The arrows show the absorbance changes upon the addition of the DNA concentrations. Insets: Linear plot of [DNA]/(ε_a-ε_f) vs. [DNA] for the titration of the Pt(II) complex (VI) with HS-DNA.

Table 4
The binding constant (K_b, M^{-1}), % hypochromicity and change in Gibb's free energy (ΔG^o, $Jmol^{-1}$) of organometallic platinum(II) complexes **(I-VI)** and 2-phenyl-5-methyl pyrazole-3-one derivatives ligands **(L^1-L^6)** with HS-DNA at different temperatures.

Compounds	λ_{max} (nm)		Δλ (nm)	K_b (M^{-1}) × 10^5	*H*%	ΔG^o ($Jmol^{-1}$)
	Bound	Free				
L^1	304	302	2	0.138	27.52	−23,617.26
L^2	385	384	1	0.172	50.55	−24,162.92
L^3	255	254	1	1.310	18.07	−29,193.11
L^4	261	259	2	0.915	17.67	−28,304.01
L^5	254	253	1	0.327	27.23	−25,754.68
L^6	257	256	1	1.410	18.58	−29,375.37
I	297	293	4	1.420	17.73	−29,392.87
II	266	261	5	1.482	22.13	−29,498.76
III	306	305	1	2.320	23.59	−30,609.14
IV	266	265	1	1.632	21.70	−29,737.63
V	263	262	1	1.500	18.65	−29,528.67
VI	266	264	2	5.580	21.78	−32,783.51

$H\% = [(A_{free} - A_{bound})/A_{free}] \times 100\%$
K_b = Intrinsic DNA binding constant determined from the UV-vis absorption spectral titration.
Δλ = Difference between bound wavelength and free wavelength.

partial intercalative mode. The magnitude of binding strength of all the compounds with HS-DNA are considered through the value of binding constant (K_b), which is calculated by monitoring changes in the absorbance at the resultant λ_{max} with increasing concentrations of HS-DNA by the Wolfe-Shimer equation [44]. The intrinsic binding constant (K_b) values of the compounds is determined by the ratio of slope and intercept in plots of [DNA]/(ε_a - ε_f) versus [DNA] (Table 4). The binding constant (K_b) values of ligands (L^1-L^6) and cyclometalated platinum(II) complexes (I-VI) are obtained in range of 0.138–1.41 × 10^5 M^{-1} and 1.42–5.58 × 10^5 M^{-1}, respectively. It's concluded that the complexes have higher binding affinity as compared to ligands. Binding constant (K_b) of the ethidium bromide is 7.1 × 10^5 M^{-1}, it is higher than synthesized compounds. The K_b values of cisplatin, oxaliplatin and carboplatin are 5.73 × 10^4 M^{-1} [45], 5.3 × 10^3 M^{-1} [46] and 0.33 × 10^3 M^{-1} [47], respectively. These K_b values are comparable to synthesized cyclometalated platinum(II) complexes and ligands. Moreover, the percentage hypochromism (*H* %) of the ligands (L^1-L^6) and complexes (I-VI) are observed in between 17.67 and 50.55% and

Table 5
Linear Stern-Volmer quenching constant (K_{sv}, M^{-1}), no. of binding sites (n) and association binding constant (K_a, M^{-1}) from calculated Stern-Volmer and Scatchard equation in fluorescence quenching analysis.

Complexes	K_{sv} (M^{-1})	K_a (M^{-1})	n	ΔG(J mol^{-1})
I	7.0 × 10^3	1.871 × 10^3	0.873	−18,667.88
II	1.55 × 10^2	2.285 × 10^3	0.8061	−19,162.49
III	2.35 × 10^2	5.80 × 10^4	1.0879	−27,174.91
IV	4.44 × 10^2	5.18 × 10^4	1.0144	−26,895.95
V	1.1 × 10^2	2.08 × 10^4	1.0837	−24,642.46
VI	3.85 × 10^2	1.71 × 10^5	1.1489	−29,855.61

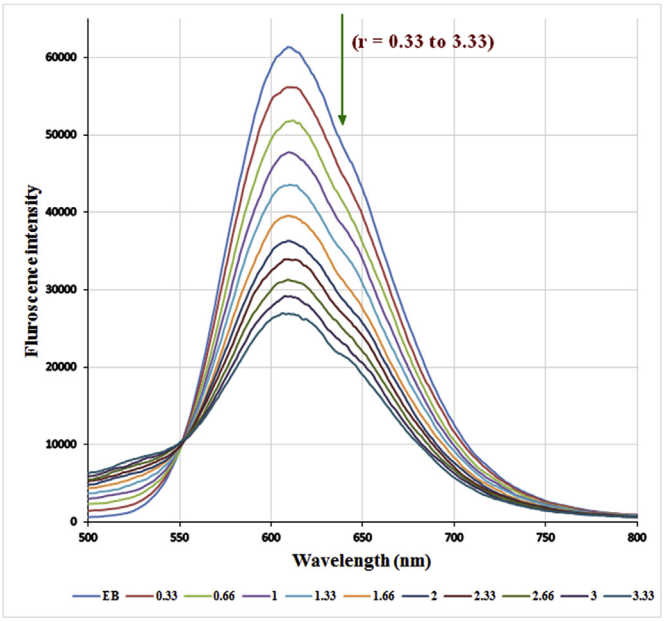

Fig. 6. Fluorescence emission spectra of ethidium bromide (EB) binds to HS-DNA in the presence of complex (IV). [EB] = 33.3 μM, [DNA] = 10 μM; [complex] = (i) 3.33, (ii) 6.66, (iii) 10, (iv) 13.33, (v) 16.66, (vi) 20, (vii) 23.33, (viii) 26.66, (ix) 30, (x) 33.3 μM; λ_{ex} = 510 nm. The arrows show the intensity changes upon increasing the concentrations of quencher (complex).

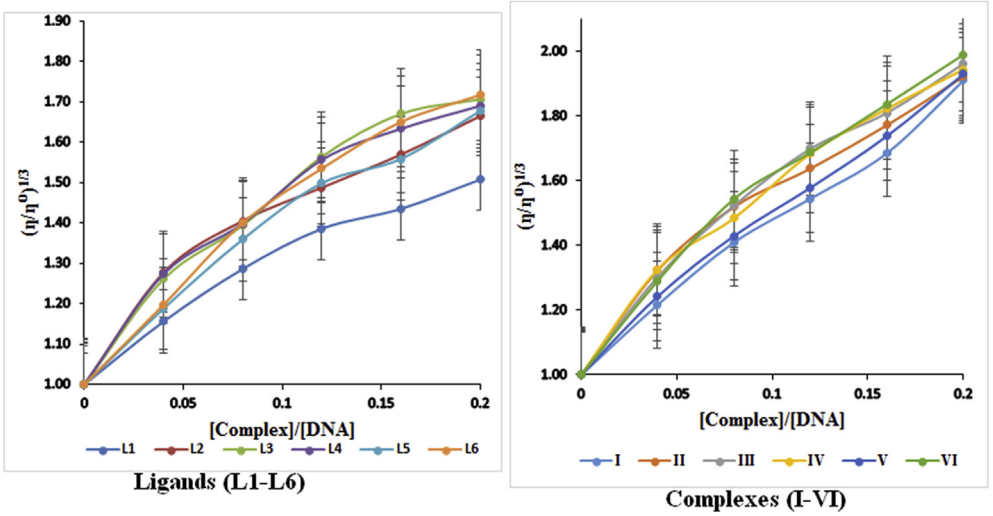

Fig. 5. Effect of increasing amounts of ligands **(L^1-L^6)** and platinum(II) complexes **(I-VI)** on the relative viscosity of HS-DNA at 27 (±0.1)°C in phosphate buffer at pH = 7.2. Error bars represent the standard deviation of three replicates.

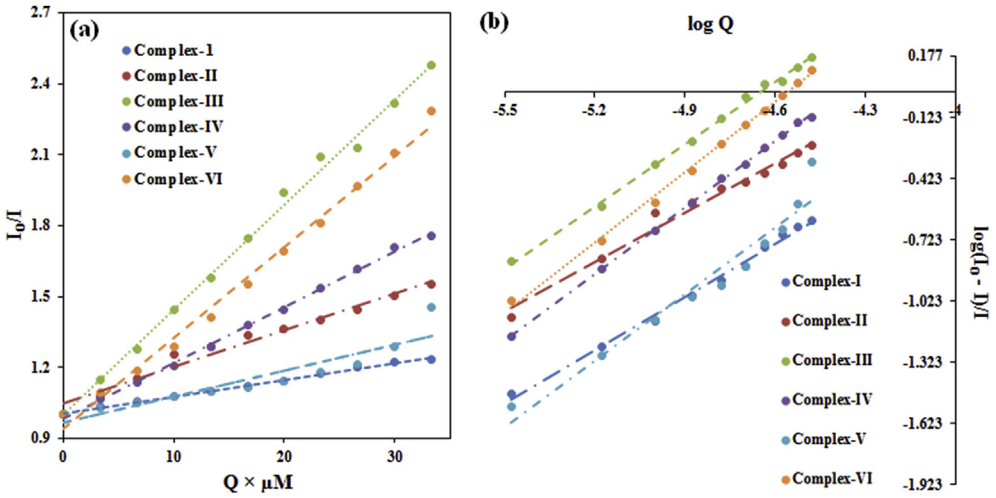

Fig. 7. The Stern-Volmer quenching graph of the EB replacement titration. (a) The Stern-Volmer quenching constant (K_{sv}) = 1.1 × 10^2 to 7.0 × 103 M^{-1}. Inset graph: plots of I_0/I versus [Q]. (b) Associative binding constant (K_a) = 1.871 × 10^3 to 1.711 × 10^5 M^{-1}. Inset graph: plot of log (I_o-I/I) versus log [Q].

17.73–23.59, respectively. The Gibb's free energy of the synthesized compounds observed values in the range of −23.62 to −32.78 kJmol^{-1} representing the spontaneity of compound-DNA binding. The binding constant values of compounds are found in the order of VI > III > IV > V > II > I > L^6 > L^3 > L^4 > L^5 > L^2 > L^1. Since, -NO_2 functional group (complex VI and ligand L^6) is a powerful electron-withdrawing group, which can accept electrons from DNA. Therefore, complex (VI) and ligand L^6 show strong binding affinity towards HS-DNA as compared to other synthesized complexes and ligands, respectively. The DNA binding data (K_b, M^{-1}, *%H* and ΔG°, Jmol^{-1}) of the synthesized compounds are represented in Table 4.

3.7.5.2. (b) Viscosity measurements. The special effects of the synthesized ligands and cyclometalated Pt(II) complexes on the relative viscosity of HS-DNA has been represented in Fig. 5. The viscosity of all the compounds is slightly increase with HS-DNA as comparable to EB, suggesting the partial intercalative mode of binding and this result is similar to the electronic absorption titration spectroscopic data. The observed relative viscosity of the synthesized ligands and complexes are in order of EB > VI > III > IV > V > II > I > L^6 > L^3 > L^4 > L^5 > L^2 > L^1.

3.7.5.3. (c) Fluorescence quenching analysis. Fluorescence quenching analysis has been carried out for cyclometalated platinum(II) complexes and the corresponding emission spectra of the EB-DNA solutions in the presence of the increasing amounts of complex concentrations (r = 0.33 to 3.33), fluorescence quenching data of all complexes and graph are represented in supplementary material 5 and Table 5. Which clearly indicate a dramatic increase in the fluorescence intensity of the EB-DNA by adding the Pt(II) complex.

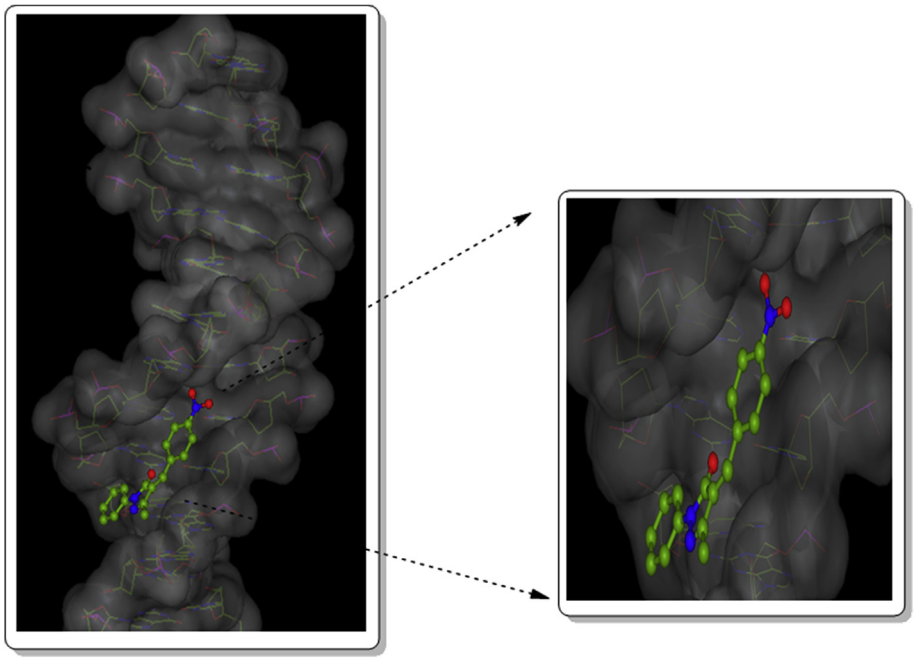

Fig. 8. Molecular docking of ligand (L^6) (ball and stick) with the DNA duplex (VDW spheres) of sequence d(ACCGACGTCGGT)$_2$.

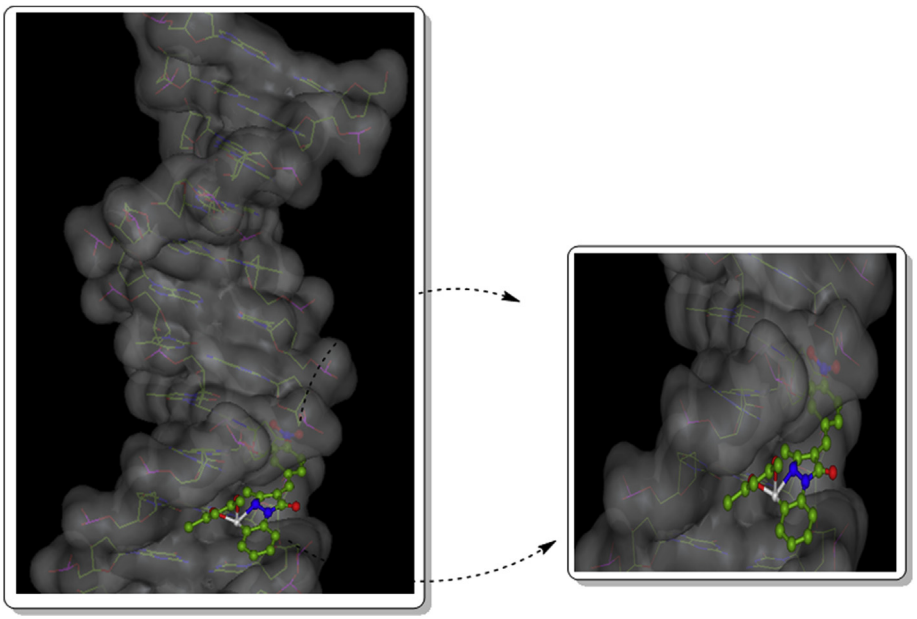

Fig. 9. Molecular docking of complex (VI) (ball and stick) with the DNA duplex (VDW spheres) of sequence d(ACCGACGTCGGT)2.

In DNA-EB system, the increase of the fluorescence intensity is due to releasing free EB molecules (Fig. 6) [29].

Moreover, the Stern-Volmer quenching constants (K_{sv}), change in standard Gibb's free energy (ΔG^{o}) and associative binding constant (K_a) of platinum(II) complexes are observed in range of 1.1×10^2 to 7.0×10^3 M^{-1}, -18.67 to −29.85 $kJmol^{-1}$ and 1.87×10^3–1.7×10^5 M^{-1}, respectively (Table 2). Fluorescence emission spectra and the Stern-Volmer quenching graph are represented in Figs. 6 and 7, respectively.

3.7.5.4. Molecular docking study. The synthesized compound can play an important role in the improvement of new chemotherapeutic drugs that lead to the recognition of specific sequences and structures of nucleoside and nucleotide [48]. Molecular docking study displays a very significant role to understanding the mechanistic pathway of complex-DNA interactions, by placing the complex penetrate binding site of the DNA helix. The ligands (L^1-L^6) and cyclometalated heteroleptic platinum(II) complexes (I-VI) are docked with in a DNA double helix structure by molecular docking study (supplementary material 6). Docked structures of ligand (L^6) and complex (VI) are represented in Fig. 8 and Fig. 9, respectively. The complexes under investigation bind with B-DNA (PDB ID: 1BNA) at the A-T rich via partial intercalation mode [49]. The binding energies of the docked ligands and cyclometalated platinum(II) complexes (I-VI) with B-DNA are represented in Table 6. The platinum(II) complexes exhibit higher binding affinity with B-DNA as compared to ligands. The compound interact with DNA, to provide greater binding affinity obtained by molecular docking study is in agreement with the experimental results developed from electronic absorption titration, viscosity measurements and fluorescence studies.

Table 6
The binding energies of the docked ligands and cyclometalated platinum(II) complexes (I-VI) with B-DNA in kJ/mol.

Ligands	Docking energy (kJ/mol)	Complexes	Docking energy (kJ/mol)
L^1	−240.74	**I**	−310.03
L^2	−253.48	**II**	−318.11
L^3	−242.21	**III**	−311.87
L^4	−243.39	**IV**	−308.29
L^5	−247.50	**V**	−296.78
L^6	−256.89	**VI**	−325.79

3.7.6. DNA nuclease study

The effect of the compounds on DNA is estimated by their DNA-cleavage ability [50,51]. Which can be determined by the cleavage mechanism. The cleavage efficiency of molecules is usually examined by agarose gel electrophoresis [52,53]. The cyclometalated platinum(II) complexes, cisplatin, transplatin and ligands are promote the percentage cleavage of pUC19 DNA from supercoiled Form I to the open circular Form II (Fig. 10). The control experiment using DNA alone does not show any significant cleavage of DNA (Lane 1). A slight cleavage is observed when K_2PtCl_4 salt has been added to

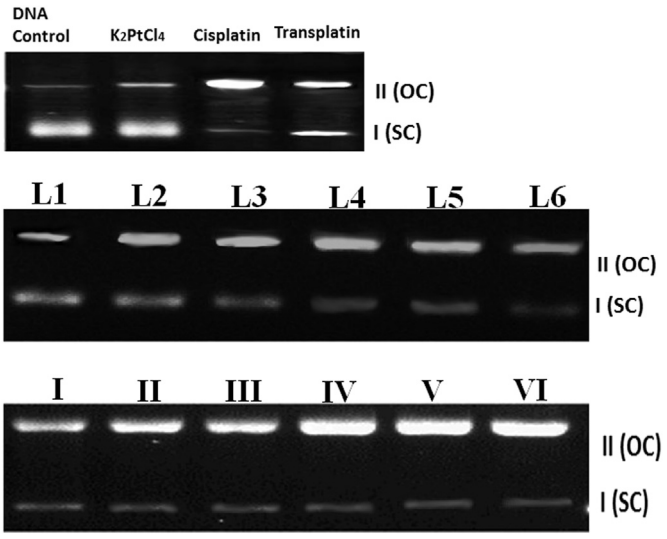

Fig. 10. Photogenic view of cleavage of pUC19 DNA (300 μg/cm^3) with ligands (L^1-L^6) and Pt(II) complexes (I-VI) using 1% agarose gel containing 0.5 μg/cm^3 EtBr. Reactions were incubated in TE buffer solution (pH = 8) at a final volume of 15 mm^3 for time period of 3 h at 37 °C.

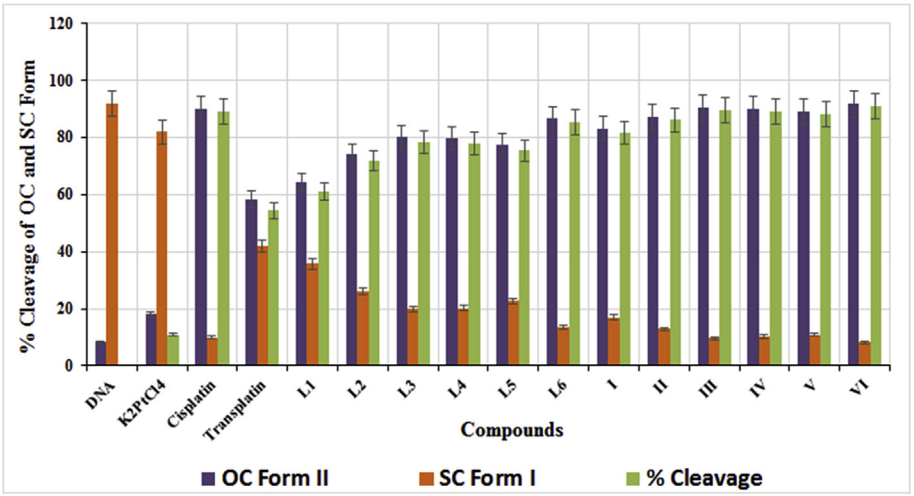

Fig. 11. Plot of nuclease cleavage activity of the ligands (L^1-L^6) and Pt(II) complexes (I-VI). Error bars represent standard deviation of three replicates (±5%).

the DNA (Lane 2). A significant cleavage of the supercoiled form to open circular form is observed, when cisplatin, transplatin and platinum(II) complexes is added to the DNA (Lane 3–9). The % cleavage for all the compounds are calculated using AlphaDigi-DocTM RT Version V.4.1.0 PC–Image software. And % cleavage data of the synthesized compounds are represented in supplementary material 9. The % cleavage ability of the compounds is in order of cisplatin > VI > III > IV > V > II > I > L^6 > L^3 > L^4 > L^5 > L^2 > L^1 > transplatin > K_2PtCl_4. The complexes (I-VI) and cisplatin exhibit greater DNA cleavage affinity as compared to ligands (L^1-L^6), transplatin and K_2PtCl_4 salt at the same concentration. Fig. 11 (supplementary material 7) represent percentage cleavage of compounds.

4. Conclusion

A series of cyclometalated platinum(II) complexes and 2-phenyl-5-methyl pyrazolone based ligands have been synthesized. The platinum(II) complexes exhibit square planar geometry and diamagnetic in nature. DNA binding activities of the synthesized compounds have been carried out using electronic absorption titration spectroscopy, fluorescence quenching analysis, viscosity measurements and molecular docking study. These studies suggest partial intercalation mode of binding. The complexes exhibit highest binding ability and binding strength as compared to ligands. The binding constant (K_b) of complex (VI) is higher than other compound because of the complex (VI) containing highly electron withdrawing functional group (-NO_2 group). The complexes and cisplatin exhibit effective DNA cleavage as compared to ligands, transplatin and K_2PtCl_4 salt. The platinum(II) complexes and cisplatin exhibit excellent *in vitro* brine shrimp cytotoxicity activity as compared to ligands and transplatin. The % viability of the platinum(II) complexes is comparable to the cisplatin and higher as compared to transplatin and ligands. The minimum inhibitory concentration of the synthesized platinum(II) complexes (I-VI) show higher potency against two Gram$^{(+ve)}$ and three Gram$^{(-ve)}$ microorganism. Further studies are necessary to evaluate precise molecular mechanism of cytotoxicity and the pharmacological properties to reveal the actual mechanism of the biological activity.

Acknowledgement

The authors are thankful to the Head, Department of Chemistry, Sardar Patel University, Vallabh Vidyanagar, Gujarat, India, for providing necessary research facilities, DST-PURSE, Sardar Patel University, Vallabh Vidyanagar for mass spectral analysis. The authors gratefully acknowledge the University Grants Commission, New Delhi, India for meritorious fellowships awarded to them during year 2014–2018 and "BSR UGC One Time Grant" (C/2013/BSR/Chemistry/7489), vide UGC letter no. F.19-119/2014 (BSR).

Appendix A. Supplementary data

Supplementary data related to this article can be found at https://doi.org/10.1016/j.jorganchem.2017.11.012.

References

[1] R. Cortés, M. Crespo, L. Davin, R. Martín, J. Quirante, D. Ruiz, R. Messeguer, C. Calvis, L. Baldomà, J. Badia, M. Font-Bardía, T. Calvet, M. Cascante, Seven-membered cycloplatinated complexes as a new family of anticancer agents. X-ray characterization and preliminary biological studies, Eur. J. Med. Chem. 54 (2012) 557–566.
[2] Y. Liu, J. Vinje, C. Pacifico, G. Natile, E. Sletten, Formation of adenine–N3/guanine–N7 cross-link in the reaction of trans-oriented platinum substrates with dinucleotides, J. Am. Chem. Soc. 124 (43) (2002) 12854–12862.
[3] J. Reedijk, The relevance of hydrogen bonding in the mechanism of action of platinum antitumor compounds, Inorg. Chim. Acta 198 (1992) 873–881.
[4] M. Nakai, F. Sekiguchi, M. Obata, C. Ohtsuki, Y. Adachi, H. Sakurai, C. Orvig, D. Rehder, S. Yano, Synthesis and insulin-mimetic activities of metal complexes with 3-hydroxypyridine-2-carboxylic acid, J. Inorg. Biochem. 99 (6) (2005) 1275–1282.
[5] A.T. Chaviara, P.C. Christidis, A. Papageorgiou, E. Chrysogelou, D.J. Hadjipavlou-Litina, C.A. Bolos, In vivo anticancer, anti-inflammatory, and toxicity studies of mixed-ligand Cu(II) complexes of dien and its Schiff dibases with heterocyclic aldehydes and 2-amino-2-thiazoline. Crystal structure of [Cu(dien)(Br)(2a-2tzn)](Br)(H2O), J. Inorg. Biochem. 99 (11) (2005) 2102–2109.
[6] P.J. Sadler, Z. Guo, Metal complexes in medicine: design and mechanism of action, Pure Appl. Chem. (1998) 863.
[7] R.A. Sanchez-Delgado, K. Lazardi, L. Rincon, J.A. Urbina, A.J. Hubert, A.N. Noels, Toward a novel metal-based chemotherapy against tropical diseases. 1. Enhancement of the efficacy of clotrimazole against Trypanosoma cruzi by complexation to ruthenium in RuCl2(clotrimazole)2, J. Med. Chem. 36 (14) (1993) 2041–2043.
[8] E.J. Trickett, C.J. Jones, Adolescent culture brokering and family functioning: a study of families from Vietnam, Cult. Divers. Ethn. Minority Psychol. 13 (2) (2007) 143–150.
[9] A.A. Bekhit, H.M.A. Ashour, Y.S. Abdel Ghany, A.E.-D.A. Bekhit, A. Baraka, Synthesis and biological evaluation of some thiazolyl and thiadiazolyl derivatives of 1H-pyrazole as anti-inflammatory antimicrobial agents, Eur. J. Med. Chem. 43 (3) (2008) 456–463.
[10] X.-H. Liu, B.-F. Ruan, J.-X. Liu, B.-A. Song, L.-H. Jing, J. Li, Y. Yang, H.-L. Zhu, X.-B. Qi, Design and synthesis of N-phenylacetyl (sulfonyl) 4,5-dihydropyrazole derivatives as potential antitumor agents, Bioorg. Med. Chem. Lett. 21 (10)

(2011) 2916–2920.
[11] T.N. Ngo, S.A. Ejaz, T.Q. Hung, T.T. Dang, J. Iqbal, J. Lecka, J. Sevigny, P. Langer, Efficient one-pot synthesis of 5-perfluoroalkylpyrazoles by cyclization of hydrazone dianions, Org. Biomol. Chem. 13 (30) (2015) 8277–8290.
[12] Y.-J. Liu, H. Chao, L.-F. Tan, Y.-X. Yuan, W. Wei, L.-N. Ji, Interaction of polypyridyl ruthenium (II) complex containing asymmetric ligand with DNA, J. Inorg. Biochem. 99 (2) (2005) 530–537.
[13] A.J.S.B.S.H. Furniss, P.W.G. Tatchell, A.R. Vogel, Vogel's Textbook of Practical Organic Chemistry, fifth ed., 2004.
[14] A. Liang, Y. Li, W. Zhu, Y. Wang, F. Huang, H. Wu, Y. Cao, Novel cyclometalated platinum (II) complex containing carrier-transporting groups: synthesis, luminescence and application in single dopant white PLEDs, Dyes Pigments 96 (3) (2013) 732–737.
[15] C.-L. Ho, W.-Y. Wong, B. Yao, Z. Xie, L. Wang, Z. Lin, Synthesis, characterization, photophysics and electrophosphorescent applications of phosphorescent platinum cyclometalated complexes with 9-arylcarbazole moieties, J. Organomet. Chem. 694 (17) (2009) 2735–2749.
[16] B.N. Meyer, N.R. Ferrigni, J.E. Putnam, L.B. Jacobsen, D.E. Nichols, J.L. McLaughlin, Brine shrimp: a convenient general bioassay for active plant constituents, Planta Med. 45 (05) (1982) 31–34.
[17] J.V. Mehta, S.B. Gajera, M.N. Patel, Biological applications of pyrazoline-based half-sandwich ruthenium(III) coordination compounds, J. Biomol. Struct. Dyn. (2016) 1–9.
[18] J. Marmur, A procedure for the isolation of deoxyribonucleic acid from microorganisms, J. Mol. Biol. 3 (2) (1961), 208–IN1.
[19] T.M.H. Paul, M.G.B. Drew, P. Chattopadhya, Synthesis, characterization, crystal structure, and DNA-binding of ruthenium(II) complexes of heterocyclic nitrogen ligands resulting from a benzimidazole-based quinazoline derivative, J. Coord. Chem. 65 (8) (2012) 1289.
[20] Yong Li, Zheng-Yin Yang, Ming-Fang Wang, Synthesis, characterization, DNA binding properties, fluorescence studies and antioxidant activity of transition metal complexes with hesperetin-2-hydroxy benzoyl hydrazone, J. Fluoresc. 20 (4) (July 2010) 891–905.
[21] S. Ramakrishnan, E. Suresh, A. Riyasdeen, M.A. Akbarsha, M. Palaniandavar, DNA binding, prominent DNA cleavage and efficient anticancer activities of Tris(diimine)iron(ii) complexes, Dalton Trans. 40 (14) (2011) 3524–3536.
[22] G. Cohen, H. Eisenberg, Viscosity and sedimentation study of sonicated DNA–proflavine complexes, Biopolymers 8 (1) (1969) 45–55.
[23] S. Mondal, B. Pakhira, A.J. Blake, M.G.B. Drew, S.K. Chattopadhyay, Co(III) and Ni(II) complexes of an anthracene appended aroyl hydrazone: synthesis, crystal structures, DNA binding and catecholase activity, Polyhedron 117 (2016) 327–337.
[24] J.R. Lakowicz, Principles of Fluorescence Spectroscopy, Springer, 2006.
[25] L. Zhu, K. Zheng, Y.-T. Li, Z.-Y. Wu, C.-W. Yan, Synthesis and structure elucidation of new μ-oxamido-bridged dicopper(II) complex with in vitro anticancer activity: a combined study from experiment verification and docking calculation on DNA/protein-binding property, J. Photochem. Photobiol. B Biol. 155 (2016) 86–97.
[26] O. Stern, M. Volmer, Z. Phys. 20 (1919) 183.
[27] R. Frank, H. Rau, Static and dynamic quenching of the emission of excited ruthenium(II) tris(bipyridyl) cation by nickel(II)-tetracyanodithiolene anion, J. Phys. Chem. 87 (25) (1983) 5181–5184.
[28] A. Kathiravan, R. Renganathan, Photoinduced interactions between colloidal TiO2 nanoparticles and calf thymus-DNA, Polyhedron 28 (7) (2009) 1374–1378.
[29] K.P. Thakor, M.V. Lunagariya, M.N. Patel, Acetyl pyridine-based palladium(II) compounds as an artificial metallonucleases, J. Biomol. Struct. Dyn. (2016) 1–13.
[30] M. Hong, G. Chang, R. Li, M. Niu, Anti-proliferative activity and DNA/BSA interactions of five mono- or di-organotin(iv) compounds derived from 2-hydroxy-N[prime or minute]-[(2-hydroxy-3-methoxyphenyl)methylidene]-benzohydrazone, New J. Chem. 40 (9) (2016) 7889–7900.
[31] M.-L. Liu, M. Jiang, K. Zheng, Y.-T. Li, Z.-Y. Wu, C.-W. Yan, Synthesis and structure of a new mononuclear copper(II) complex with 2,2′-bipyridine and picrate: molecular docking, DNA-binding, and in vitro anticancer activity, J. Coord. Chem. 67 (4) (2014) 630–648.
[32] D. Sinha, A.K. Tiwari, S. Singh, G. Shukla, P. Mishra, H. Chandra, A.K. Mishra, Synthesis, characterization and biological activity of Schiff base analogues of indole-3-carboxaldehyde, Eur. J. Med. Chem. 43 (1) (2008) 160–165.
[33] V.X. Jin, J.D. Ranford, Complexes of platinum(II) or palladium(II) with 1,10-phenanthroline and amino acids, Inorg. Chim. Acta 304 (1) (2000) 38–44.
[34] H. Li, J. Ding, Z. Xie, Y. Cheng, L. Wang, Synthesis, characterization and electrophosphorescent properties of mononuclear platinum(II) complexes based on 2-phenylbenzoimidazole derivatives, J. Organomet. Chem. 694 (17) (2009) 2777–2785.
[35] A.A. Soliman, O.I. Alajrawy, F.A. Attaby, W. Linert, New binary and ternary platinum(II) formamidine complexes: synthesis, characterization, structural studies and in-vitro antitumor activity, J. Mol. Struct. 1115 (2016) 17–32.
[36] P.R. Reddy, A. Shilpa, Oxidative and hydrolytic DNA cleavage by Cu(II) complexes of salicylidene tyrosine schiff base and 1,10 phenanthroline/bipyridine, Polyhedron 30 (4) (2011) 565–572.
[37] C. Shiju, D. Arish, N. Bhuvanesh, S. Kumaresan, Synthesis, characterization, and biological evaluation of Schiff base–platinum(II) complexes, Spectrochim. Acta Part A Mol. Biomol. Spectrosc. 145 (2015) 213–222.
[38] R. Prabhakaran, A. Geetha, M. Thilagavathi, R. Karvembu, V. Krishnan, H. Bertagnolli, K. Natarajan, Synthesis, characterization, EXAFS investigation and antibacterial activities of new ruthenium(III) complexes containing tetradentate Schiff base, J. Inorg. Biochem. 98 (12) (2004) 2131–2140.
[39] B.G. Tweedy, Phytopathology 55 (1964) 910.
[40] P. Kalaivani, R. Prabhakaran, F. Dallemer, P. Poornima, E. Vaishnavi, E. Ramachandran, V.V. Padma, R. Renganathan, K. Natarajan, DNA, protein binding, cytotoxicity, cellular uptake and antibacterial activities of new palladium(ii) complexes of thiosemicarbazone ligands: effects of substitution on biological activity, Metallomics 4 (1) (2012) 101–113.
[41] N.R.F.B.N. Meyer, J.E. Putnam, L.B. Jacobsen, D.E. Nichols, J.L. McLaughlin, Brine shrimp: a convenient general bioassay for active plant constituents, Planta Med. 45 (1982) 31–34.
[42] E.-J. Gao, F. Hong, M.-C. Zhu, C. Ma, S.-K. Liang, J. Zhang, L.-F. Li, L. Wang, Y.-Y. Li, J. Wei, Effect of carbon chain length on biological activity of novel palladium (II) complexes, Eur. J. Med. Chem. 82 (2014) 172–180.
[43] C. Janiak, A critical account on [small pi]-[small pi] stacking in metal complexes with aromatic nitrogen-containing ligands, J. Chem. Soc. Dalton Trans. 21 (2000) 3885–3896.
[44] C. Protogeraki, E.G. Andreadou, F. Perdih, I. Turel, A.A. Pantazaki, G. Psomas, Cobalt(II) complexes with the antimicrobial drug enrofloxacin: structure, antimicrobial activity, DNA- and albumin-binding, Eur. J. Med. Chem. 86 (2014) 189–201.
[45] J. Liu, W. Zheng, S. Shi, C. Tan, J. Chen, K. Zheng, L. Ji, Synthesis, antitumor activity and structure–activity relationships of a series of Ru(II) complexes, J. Inorg. Biochem. 102 (2) (2008) 193–202.
[46] C.N. N'Soukpoé-Kossi, C. Descôteaux, É. Asselin, H.-A. Tajmir-Riahi, G. Bérubé, DNA interaction with novel antitumor estradiol–platinum(ii) hybrid molecule: a comparative study with cisplatin drug, DNA Cell Biol. 27 (2) (2007) 101–107.
[47] H. Soori, A. Rabbani-Chadegani, J. Davoodi, Exploring binding affinity of oxaliplatin and carboplatin, to nucleoprotein structure of chromatin: spectroscopic study and histone proteins as a target, Eur. J. Med. Chem. 89 (2015) 844–850.
[48] A. Paul, S. Anbu, G. Sharma, M.L. Kuznetsov, B. Koch, M.F.C. Guedes da Silva, A.J.L. Pombeiro, Synthesis, DNA binding, cellular DNA lesion and cytotoxicity of a series of new benzimidazole-based Schiff base copper(ii) complexes, Dalton Trans. 44 (46) (2015) 19983–19996.
[49] D.R. Boer, A. Canals, M. Coll, DNA-binding drugs caught in action: the latest 3D pictures of drug-DNA complexes, Dalton Trans. 3 (2009) 399–414.
[50] J.-G. Liu, Q.-L. Zhang, X.-F. Shi, L.-N. Ji, Interaction of [Ru(dmp)2(dppz)]2+ and [Ru(dmb)2(dppz)]2+ with DNA: effects of the ancillary ligands on the DNA-binding behaviors, Inorg. Chem. 40 (19) (2001) 5045–5050.
[51] A.M. Pyle, J.P. Rehmann, R. Meshoyrer, C.V. Kumar, N.J. Turro, J.K. Barton, Mixed-ligand complexes of ruthenium(II): factors governing binding to DNA, J. Am. Chem. Soc. 111 (8) (1989) 3051–3058.
[52] J. Qian, W. Gu, H. Liu, F. Gao, L. Feng, S. Yan, D. Liao, P. Cheng, The first dinuclear copper(ii) and zinc(ii) complexes containing novel Bis-TACN: syntheses, structures, and DNA cleavage activities, Dalton Trans. 10 (2007) 1060–1066.
[53] B. Macías, M.V. Villa, B. Gómez, J. Borrás, G. Alzuet, M. González-Álvarez, A. Castiñeiras, DNA interaction of new copper(II) complexes with sulfonamides as ligands, J. Inorg. Biochem. 101 (3) (2007) 444–451.